

# Halogen Enabled Aqueous Flow Cells for Large-Scale Energy Storage: Current

## Status and Perspectives

Jiayi Li, Zeyu Xu, Maochun Wu\*

*Department of Mechanical Engineering, The Hong Kong Polytechnic University,*

*Hong Kong SAR 999077, China*

\* Corresponding author.

*E-mail address:* maochun.wu@polyu.edu.hk (M.C. Wu).

## Abstract

Aqueous flow cells, including redox flow batteries and regenerative fuel cells, are promising technologies for grid-scale energy storage due to their intrinsic safety, high scalability, and flexibility in decoupling power and energy. Redox active species are critical components of aqueous flow cells as they largely determine the energy density, cell performance, and system cost. Halogens have attracted enormous interest as redox active species for aqueous flow cells due to their low cost, high natural abundance, and desirable electrochemical properties, such as high redox potential and high reversibility. Moreover, halogen species have been widely used as redox mediators and complexing agents to improve the reversibility and solubility of active materials, enabling aqueous flow cells to achieve high energy density and performance. This review provides a comprehensive summary of various types of aqueous flow cells that use halogens as active materials, redox mediators, and complexing agents. The working principles, critical issues, and recent progress are systematically discussed based on the roles and types of halogen species. Finally,

existing challenges and future perspectives on halogen-based flow cells are highlighted.

**Keywords:** Redox flow batteries; regenerative fuel cells; halogens; redox mediator; energy storage

## 1. Introduction

As the world grapples with the dual challenge of increasing energy demand and environmental concerns, the need for clean and renewable energy sources has become more pressing than ever [1–4]. While the technologies capable of generating electricity from various renewable energy sources, such as solar and wind, have dramatically advanced in recent decades, the intermittent and uncontrollable nature of these renewables makes it challenging to integrate them into the existing electric grid [5–7]. Large-scale energy storage systems that can efficiently store and release electricity to smooth out the intermittency provide a promising solution to this grand challenge [8,9]. Among all possible technologies, aqueous flow cells, including redox flow batteries (RFBs) and regenerative fuel cells, represent one of the promising candidates for this application. Typically, a flow cell consists of an electrochemical cell and two external tanks. Unlike conventional rechargeable batteries where electroactive materials are packed and sealed in the cell, the active materials in flow cells are stored in external tanks, which are circulated to the electrochemical cell for energy conversion. This unique design allows for the decoupling of the energy and power of a system, rendering it possible to independently adjust the storage capacity and power output to meet the requirements of particular applications. Furthermore,

the electrodes in redox flow cells only provide active sites for electrochemical reactions during charging and discharging processes [10]. Therefore, they are free from physicochemical change and mechanical stress, giving flow cells a long service life. In addition to these unique features, aqueous flow cells also exhibit other attractive characteristics, including site-independency, intrinsic safety, high efficiency, high design flexibility, and fast response [11], making them particularly suitable for large-scale energy storage.

For a flow cell, redox couples, or redox active species, play a decisive role in determining the cost, energy density and electrochemical performance, including power density, energy efficiency (EE) and cycle life [12,13]. Generally, the redox active species should meet the following requirements: (1) Suitable redox potential. The positive and negative redox couples should respectively display a high and low redox potential to widen the cell voltage without causing parasitic reactions, such as hydrogen evolution reaction (HER) and oxygen evolution reaction (OER). (2) High electrochemical reactivity, reversibility, and stability. These properties are essential to achieve high power density, high efficiency, and long life. (3) High solubility to attain a high energy density. (4) Environmental friendliness. (5) Abundant resources and low cost. Although a wide variety of redox couples have been reported so far, few of them can meet all the above requirements. Currently, vanadium redox couples ( $V^{3+}/V^{2+}$  and  $VO_2^+/VO^{2+}$ ) are the most widely used redox active species and the resulting flow batteries are called all vanadium RFBs (VRFBs) [14–18]. Because of their free of contamination, high EE, and long cycle life, VRFBs have attracted the most attention

and are nowadays at the stage of commercial demonstration [19–22]. However, broader market penetration of this technology is severely hindered by two critical challenges: relatively low energy density and high cost [23]. The former results from the poor solubility of vanadium species in sulfuric acid solutions (usually 1.6–2.0 M) while the latter is mainly due to the use of expensive vanadium species [14,23–25]. It is estimated that electrolyte accounts for about 37–63% of the capital cost of the VRFB systems [15,18,26]. Therefore, considerable efforts have been made to develop novel redox couples at low cost. Of possible candidates, halogen-based redox couples (i.e.,  $\text{Cl}_2/\text{Cl}^-$ ,  $\text{Br}_2/\text{Br}^-$ , and  $\text{I}_3^-/\text{I}^-$ ) are promising alternatives to vanadium species because of their abundant resources, low cost, and decent electrochemical properties [4]. Over the past decades, a wide range of halogen-based RFBs have been developed by pairing with various negative redox couples, such as  $\text{Zn}^{2+}/\text{Zn}$ ,  $\text{V}^{3+}/\text{V}^{2+}$ ,  $\text{H}^+/\text{H}_2$ , and  $\text{S}_2^{2-}/\text{S}^{2-}$  [27–30]. Among them, zinc-bromine flow batteries (ZBFBs) are the most developed and several pilot plants have been demonstrated. For example, a 2 MW/2 MWh system for load leveling service was constructed by ZBB technologies (now Ensyntax Energy systems, US) [31], showing great promise of halogen-based RFBs for practical applications. Moreover, some halide redox couple (e.g.,  $\text{I}_3^-/\text{I}^-$ ) can be used as redox mediators to enable novel flow cell designs, such as redox targeting RFBs and solar rechargeable RFBs [32–34], providing new opportunities for the development of RFBs with high energy density. In addition, halide ions can complex with elementary halogens (e.g.,  $\text{I}_2$  and  $\text{Br}_2$ ) and other active redox active species (e.g., vanadium ions) to achieve higher solubility, stability, and reversibility, thereby enhancing the energy

density and performance of RFBs.

In this review, we aim to provide a comprehensive summary of the history and recent progress in the development of aqueous flow cells that utilize halogen species as active redox couples, redox mediators, and complexing agents (**Fig. 1**). Advances in key components including electrolytes, electrodes, and membranes to improve the performance of these halogen enabled flow cells are highlighted. Finally, remaining challenges and prospects for future development are discussed.

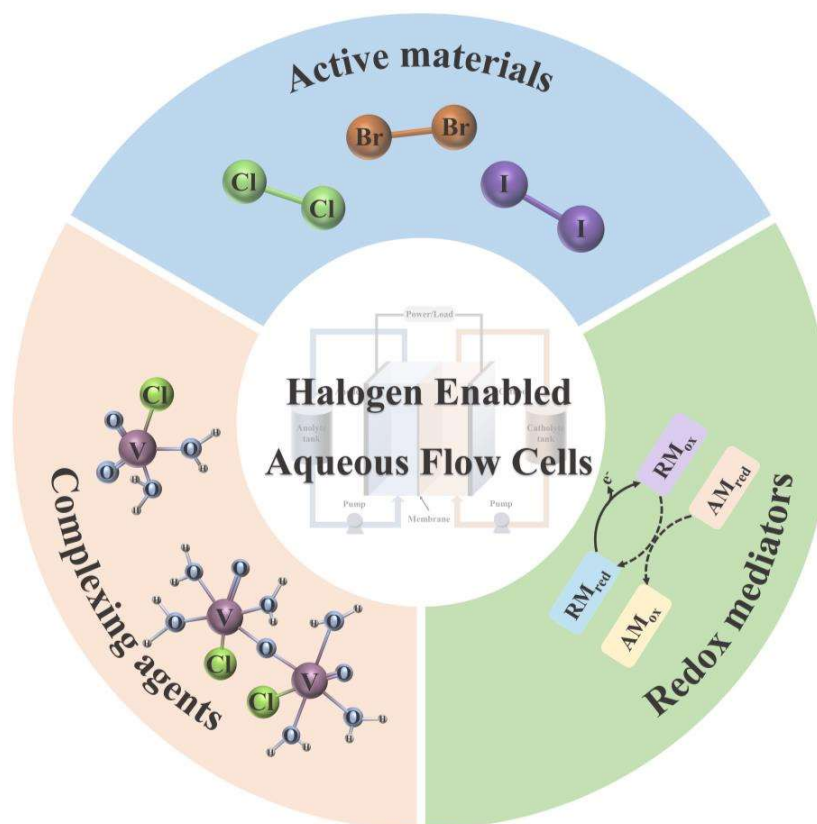


**Fig. 1.** Overview of halogens as active materials, redox mediators, and complexing agents in aqueous flow cells.

## 2. Methodology

In this review, almost all available research works on flow batteries and

regenerative fuel cells that use halogens (i.e., chlorine, bromine, and iodine) are identified. The literature research is carried out in the online databases Scopus and Web of Science using the following search strategies:

Scopus: Article title, Abstract, Keywords (aqueous flow battery OR aqueous flow cell OR regenerative fuel cell) AND Article title, Abstract, Keywords (halogen OR chlorine OR bromine OR and iodine), OR Article title, Abstract, Keywords (hydrogen-halogen regenerative fuel cell), OR Article title, Abstract, Keywords (zinc-halogen flow battery), OR Article title, Abstract, Keywords (redox mediator OR redox target) AND Article title, Abstract, Keywords (halogen OR chlorine OR bromine OR iodine) AND Article title, Abstract, Keywords (aqueous flow battery), OR Article title, Abstract, Keywords (complexing agent OR sequestering agent) AND Article title, Abstract, Keywords (aqueous flow battery)

Web of Science: Topic: (halogen flow battery) OR Topic: (halogen regenerative fuel cell) OR Topic: (chlorine-based flow battery) OR Topic: (chlorine-based regenerative fuel cell) OR Topic: (bromine-based flow battery) OR Topic: (bromine-based regenerative fuel cell) OR Topic: (iodine-based flow battery).

In addition, a supplementary search is conducted using the ((aqueous flow battery OR regenerative fuel cell) AND (halogen OR chlorine OR bromine OR iodine)) search terms of the academic search engine Google Scholar.

From the lists of results, all aqueous flow cells using halogen species as positive active materials, redox mediators and complexing agents are considered. Papers that focus on addressing the issues of negative redox reactions are not proposed, because

1 this work primarily focuses on the role of halogens. The relevant studies are classified  
2  
3 by the three roles of halogens in aqueous flow cells, i.e., active materials, redox  
4  
5 mediators, and complexing agents. A comprehensive and in-depth summary of  
6  
7 halogen-based RFBs reported in the literature are analyzed according to the paired  
8  
9 negative redox couples. In each type of flow cells, the electrolyte formulation,  
10  
11 membrane engineering, electrode modifications, and special structure designs for  
12  
13 improving the battery performance are categorized and discussed systematically.  
14  
15 Significant electrochemical parameters including coulombic efficiency (CE), EE,  
16  
17 power density, and cycle life are compared and summarized to evaluate the properties  
18  
19 of aqueous flow cells with different components. Finally, the remaining challenges,  
20  
21 possible solutions, and perspectives are highlighted, which are expected to provide  
22  
23 useful suggestions and practical approaches for developing high-performance halogen  
24  
25 enabled aqueous flow cells for grid-scale energy storage.  
26  
27

### 28 **3. Halogens as active materials**

#### 29 **3.1 Chlorine-based flow cells**

30 Although chlorine possesses advantages of fast reaction kinetics, high abundance, low  
31  
32 cost and high redox potential, research on chlorine-based flow cells has been shelved  
33  
34 in the last century due to environmental and safety concerns, as well as other  
35  
36 intractable issues. However, some recent novel designs in chlorine-based flow  
37  
38 batteries may provide possibilities for future development.  
39  
40

##### 41 **3.1.1 Zn-Cl<sub>2</sub> flow batteries**

42 Zinc-chlorine (Zn-Cl<sub>2</sub>) flow batteries were first reported for utilization in an  
43  
44

airship in 1884 with an open circuit voltage of 2.12 V [35,36]. Typically, a Zn-Cl<sub>2</sub> flow battery consists of a Zn electrode and a porous graphite chlorine electrode in ZnCl<sub>2</sub> aqueous electrolyte [37,38]. To manage the toxic Cl<sub>2</sub> gas, Philip C. Symons invented an innovative system in 1973 [39]. As displayed in **Fig. 2a**, during charging process, Zn is deposited at the negative electrode while chloride ions are oxidized at the positive electrode to generate Cl<sub>2</sub> gas. The evolved Cl<sub>2</sub> is transferred to another storage tank where it is dissolved in water and cooled to form crystalline solid chlorine hydrates (Cl<sub>2</sub> · xH<sub>2</sub>O) [40]. During discharging process, the chlorine gas is produced by heating the chlorine hydrates, transported to the positive electrode, and reduced back to Cl<sup>-</sup> ions, while Zn anode dissolves into the electrolyte. In 1970s and 1980s, many tests were conducted to evaluate the potential of Zn-Cl<sub>2</sub> flow battery systems for a wide range of applications including electric vehicles. A test car powered by this battery system was built and travelled 152 miles at a steady speed of 50 miles per hour in 1973 [41]. In addition, in the late 1980s, the performance of 10 kW-class Zn-Cl<sub>2</sub> flow batteries was tested for electrical energy storage in Japan and there was no significant performance degradation after 1500 cycles in nearly a year [42,43]. Although Zn-Cl<sub>2</sub> flow batteries exhibit high energy density and high efficiency, they require complex auxiliary systems to manage the toxic chlorine gas. Moreover, due to the risk of leakage during battery operation, as well as possible explosion hazards caused by hydrogen evolution at the Zn electrode, Zn-Cl<sub>2</sub> flow batteries were abandoned for further development after 1980s [40,44,45].

### 3.1.2 H<sub>2</sub>-Cl<sub>2</sub> regenerative fuel cells



Hydrogen-chlorine ( $\text{H}_2\text{-Cl}_2$ ) regenerative fuel cells are another type of electrical energy storage system that is more widely studied than the phased-out  $\text{Zn-Cl}_2$  flow batteries [46]. In a  $\text{H}_2\text{-Cl}_2$  regenerative fuel cell, hydrogen and chlorine serve as the reactant gases and an aqueous  $\text{HCl}$  solution is used as the electrolyte [47]. The discharge process is akin to  $\text{H}_2\text{-O}_2$  fuel cells only by replacing  $\text{O}_2$  with  $\text{Cl}_2$  and thus the product is  $\text{HCl}$ . When being charged,  $\text{HCl}$  is electrochemically regenerated to  $\text{H}_2$  and  $\text{Cl}_2$  at the negative and positive electrodes respectively. In fact, this technology was originally proposed as an alternative to  $\text{H}_2\text{-O}_2$  regenerative fuel cells [48]. Compared with  $\text{O}_2$ ,  $\text{Cl}_2$  electrode exhibits a lower activation overpotential and higher exchange current density during charging and discharging processes because of the relatively facile redox kinetics, thus offering higher power densities and round-trip energy efficiencies [35,49]. In addition, the  $\text{H}_2\text{-Cl}_2$  cell exhibits a higher open circuit voltage of 1.36 V at normal temperature and pressure. Because of the high power density, high energy density, and use of abundant and low-cost materials,  $\text{H}_2\text{-Cl}_2$  regenerative fuel cells show great potential for grid-scale electrical energy storage. More importantly, they can also be used for industrial applications. For example, they can simultaneously generate electricity and chemicals for other production lines, such as chlor-alkali industry and electrolysis process of magnesium and sodium, with benefits for energy saving [50]. Early studies of the  $\text{H}_2\text{-Cl}_2$  regenerative fuel cells were mainly conducted by the research group in Brookhaven National Laboratory [51–53]. They systematically investigated the effects of temperature, electrolyte concentration, flow rate, flow field and electrode material on cell performances and

found that these factors had negligible effects on the open-circuit voltage [51]. In contrast, the mass transport of chlorine from the gas to the liquid phase can be facilitated by increasing the operating pressure due to the increased solubility. In addition, the use of flow-through electrodes can also significantly improve the cell performances, leading to a high electric-electric efficiency of over 75% [53].

Although the  $\text{Cl}_2/\text{Cl}^-$  redox couple displays more facile reaction kinetics than oxygen does, catalysts are still needed to accelerate the conversion rates of chloride species for practical operation. Platinum (Pt) is one of the most commonly used catalysts in fuel cells, mainly due to its high catalytic activity and stability [54]. However, Yeo et al. [53] found that corrosion of Pt electrode still occurred by half-cell measurements because the chlorine electrode potential is 0.27 V higher than that of  $\text{Pt}/\text{PtCl}_4^-$ . Thomassen et al. [55] also evaluated the performance of a  $\text{H}_2\text{-Cl}_2$  regenerative fuel cell and concluded that Pt was not stable as the electrocatalyst for chlorine reduction reactions due to the dissolution of Pt in the presence of  $\text{Cl}_2$ , forming chloroplatinic acid ( $\text{H}_2\text{PtCl}_6$ ). For this reason, using only Pt catalyst is not feasible in a  $\text{H}_2\text{-Cl}_2$  fuel cell system. Shibli and Noel [56] explored the use of bimetallic platinum-iridium-loaded catalyst (2.5 wt% Pt and 5 wt% Ir) to improve both chlorine reduction and hydrogen evolution reactions. It was demonstrated that the bimetallic catalyst exhibited much improved stability and enabled the  $\text{H}_2\text{-Cl}_2$  fuel cell to cycle stably for 300 h without significant degradation at the current density of  $100 \text{ mA cm}^{-2}$ . In addition to Pt and its alloys, ruthenium oxide ( $\text{RuO}_2$ ) was also considered as a promising catalyst for  $\text{Cl}_2/\text{Cl}^-$  reactions due to its high activity and

1 relatively lower cost than Pt [54]. However, the activity of Ru-based catalysts  
2  
3 decreases due to the oxidation during long-term operation. To improve the  
4  
5 electrocatalytic performance, Mondal and co-workers synthesized Co-Ru and Mn-Ru  
6  
7 alloy oxides by wet chemical synthesis methods [50]. The resulting alloy oxides with  
8  
9 very low noble metal content ( $\text{Co}_{0.89}\text{Ru}_{0.11}\text{O}_x$  and  $\text{Mn}_{0.99}\text{Ru}_{0.01}\text{O}_x$ ) exhibited good  
10  
11 catalytic activity for chlorine redox reactions and stability in acidic and corrosive  
12  
13 environments. Moreover, based on the previous model [57], a high-performance  
14  
15  $\text{H}_2\text{-Cl}_2$  regenerative fuel cell was developed with a chlorine electrode using an  
16  
17 electrocatalyst ( $\text{Ru}_{0.09}\text{Co}_{0.91}$ ) $_3\text{O}_4$  with low noble metal content [58]. The cell was  
18  
19 capable of delivering a peak galvanic power density of over  $1 \text{ W cm}^{-2}$  and running at  
20  
21  $0.4 \text{ W cm}^{-2}$  with a voltage efficiency (VE) of 90%, showing great promise for  
22  
23 grid-scale electrical energy storage.  
24  
25

26  
27  
28 In addition to electrodes, membranes also play a key role in  $\text{H}_2\text{-Cl}_2$  flow cells,  
29  
30 which needs to meet stringent requirements in the corrosive and acidic environment  
31  
32 due to the presence of HCl and  $\text{Cl}_2$  [59]. HCl is a highly hygroscopic chemical that  
33  
34 can remove most of the water from the membrane even under high humidification,  
35  
36 resulting in increased membrane resistance and reduced cell performances [60]. To  
37  
38 solve this problem, Liu et al. [60–62] prepared a series of composite membranes for  
39  
40  $\text{H}_2\text{-Cl}_2$  fuel cells. For example, they developed an ultrafiltration-based  
41  
42 proton-conductive membrane (UF-based PCM) consisting of polyethersulfone (PES)  
43  
44 and nanosized  $\text{SiO}_2$ . The addition of  $\text{SiO}_2$  can increase the porosity of membrane with  
45  
46 smaller pore size and enhance absorption of the aqueous acid. Therefore, this unique  
47  
48  
49  
50  
51  
52  
53  
54  
55  
56  
57  
58  
59  
60  
61  
62  
63  
64  
65

membrane structure is conducive to maintaining high proton conductivity while effectively preventing the crossover of chlorine [60]. Afterwards, they further blended PES with sulfonated poly(ether ether ketone) (SPEEK) in the UF-based PCM to increase the ionic conductivity and selectivity. It was shown that the incorporation of SPEEK with abundant  $-SO_3H$  groups can provide more proton migration sites and decrease the pore size of membrane, which can facilitate the proton transport while reducing fuel permeability. As a result, the fuel cells assembled with the optimal composite membrane could deliver a maximum power density of  $571.2 \text{ mW cm}^{-2}$ , which was 1.5 times higher than that with Nafion 212 membrane [61].

### 3.1.3 Other chlorine-based flow battery

There have been few reports of the use of  $Cl_2/Cl^-$  redox couple in RFBs in recent years, primarily due to the extreme toxicity and corrosiveness of chlorine gas. Very recently, Hou et al. [63] proposed a novel reversible membrane-free chlorine redox flow battery. As shown in **Fig. 2b**, this new chlorine-based RFB operates through electrolyzing saturated aqueous sodium chloride solutions ( $NaCl/H_2O$ ) and storing the resulting  $Cl_2$  in water-insoluble organic phases, such as carbon tetrachloride ( $CCl_4$ ) or other liquids with high  $Cl_2$  solubility that are immiscible with aqueous solution. The immiscibility between  $CCl_4$  and  $NaCl$  electrolyte enables a membrane free design, which can potentially reduce the system cost as ion-conducting membranes usually take up a large proportion of the system cost of RFBs. By pairing with a  $Na_3Ti_2(PO_4)_3$  negative electrode, the battery can deliver an energy density of up to  $125.7 \text{ Wh L}^{-1}$  and EE of higher than 91% at the current density of  $10 \text{ mA cm}^{-2}$ . Together with the

low cost of active materials and promising electrochemical performances, this work opens up new opportunities for the development of  $\text{Cl}_2$ -based flow batteries. For example, other water-immiscible organic phases that have higher  $\text{Cl}_2$  solubility can be developed to replace  $\text{CCl}_4$ , which poses environmental and safety concerns. However, the leakage of  $\text{Cl}_2$  gas remains a critical concern when scaling up, which requires further investigations.

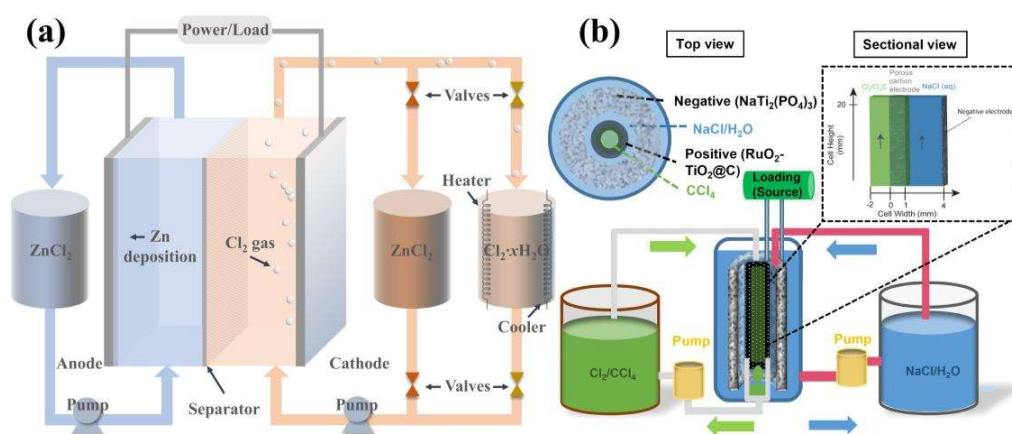


**Fig. 2.** (a) Schematic of a Zn- $\text{Cl}_2$  flow battery during charging process. (b) Schematic of the membrane-free chlorine-based redox flow battery. Reproduced with permission from Ref. [63]. Copyright 2022, Springer Nature.

Overall, despite the advantages of  $\text{Cl}_2/\text{Cl}^-$  redox couple, the practical implementation of chlorine-based flow cells has been hindered by the involvement of toxic chlorine gas. Although experience can be borrowed from chlor-alkali industry, managing chlorine at a grid-scale remains a great challenge. Therefore, efforts have been shifted to its bromine and iodine counterparts, which are discussed in the following sections.

## 3.2 Bromine-based flow cells

$\text{Br}_2/\text{Br}^-$  redox couple is the most commonly used halogens owing to its high electrode potential, high solubility, abundance of sources and low price. More importantly, bromine exists as a liquid phase at room temperature in comparison to the gaseous chlorine, which greatly reduces the complexity of the system and thus makes the bromine-based RFB more practical. Earlier bromine-based flow battery systems include ZBFBs,  $\text{H}_2\text{-Br}_2$  flow batteries, polysulfide- $\text{Br}_2$  flow batteries, and V- $\text{Br}_2$  flow batteries. Recently, a variety of novel bromine-based flow batteries have been proposed as displayed in **Fig. 3a**. This section summarizes and discusses the recent advances in these bromine-based flow cells.

### 3.2.1 Zn- $\text{Br}_2$ flow batteries

The concept of ZBFBs was first patented by Bradley in 1885 [64] and is currently the most studied bromine-based flow batteries. In ZBFB,  $\text{ZnBr}_2$  solutions are used as both the positive and negative electrolytes, which eliminates the cross-contamination issue [65]. Usually, sodium or potassium chloride is added as a supporting electrolyte to improve ionic conductivity of the electrolyte [66]. During charging process,  $\text{Br}^-$  is oxidized to  $\text{Br}_2$  in the positive electrode and  $\text{Zn}^{2+}$  is reduced to metallic Zn at negative electrode, while reversed reactions take place at the corresponding electrodes during discharging process, giving the battery a high theoretical voltage of 1.85 V.

Thus far, several ZBFB pilot plants have been demonstrated in the United States, Japan, Australia and other countries [66–68]. For example, Meidensha Corporation installed a 1 MW/4 MWh ZBFB system in Japan in the 1990s, which is the largest

ZBFB system installed to date, with a system EE of 65.9% after 1300 cycles [69,70].

In the United States, Ensync Energy installed a 500 kWh ZBFB energy storage demonstration system at the Illinois Institute of Technology for microgrids. Vionx Energy manufactured a 0.5 MW/3 MWh ZBFB energy storage system in Massachusetts, which played the role of peak regulation in 2016 [27]. Although commercial demonstrations have been achieved, ZBFBs still face several critical challenges, including Zn dendrite formation, Br<sub>2</sub> crossover and corrosiveness, low operating current density, and low EE. To address these challenges, tremendous efforts have been made and the performance of ZBFBs has been greatly improved. The electrochemical performances of recently reported ZBFBs are summarized and compared in **Table S1**. It should be noted that this review mainly focuses on the Br<sub>2</sub> side. Therefore, strategies to tackle Zn dendrite formation are not presented. Readers interested in this topic can refer to relevant review articles [71–77].

#### 2.2.1.1 Electrolyte formulation

Tailoring the electrolyte composition represents one of the most straightforward and effective strategies to address the issues of Br<sub>2</sub> crossover and corrosiveness. For example, bromine complexing agents (BCAs) are commonly added into the electrolyte to complex with bromine, which can effectively reduce the Br<sub>2</sub> vapor pressure and lower the Br<sub>2</sub> concentration in the aqueous solution, thus greatly reducing the reactivity of Br<sub>2</sub> and mitigating Br<sub>2</sub> crossover. Moreover, the resulting bromine complexes usually exhibit a larger molecular size, which makes it more difficult to permeate the membrane and thus further alleviates Br<sub>2</sub> crossover [78].

Cathro et al. [79] screened various cyclic and aliphatic quaternary ammonium bromides (QBr), such as N-ethyl-N-methylmorpholinium bromide (EMMB), N-chloromethyl-N-methyl-pyrrolidinium bromide (CMPB), N-ethyl-N-methylmorpholinium bromide (MEMBr), N-ethyl-N-methyl pyrrolidinium bromide (MEPBr) and their mixtures for ZFBFs. They found that the use of MEPBr and MEMBr in a molar ratio of 1:1 provided a stable complexation effect and extended the operating temperature range of the system [79]. After complexation, the larger organic cations of these complexing agents are transformed into a denser oily phase while the complex droplets attached to the electrode surface can also increase the bromine reduction current [80,81]. In addition, Schneider et al. [82] evaluated five alternative bromine sequestering agents (BSAs) for ZFBFs and found that 1-ethylpyridinium bromide ([C<sub>2</sub>Py]Br) and 1-ethyl-3-methylimidazolium bromide ([C<sub>2</sub>MIm]Br) could improve the cycle performance of ZFBFs compared to the other candidates studied. It should be noted that the addition of excessive BCAs will decrease the electrolyte conductivity, thereby increasing the polarization of the battery. Therefore, the amount of BCAs should be controlled within an appropriate range. Note that the existence of an immiscible polybromide phase requires a complex network of piping and control system to ensure the access of electroactive materials during discharge process. To solve this issue, Bryans et al. [83] proposed three novel quaternary ammonium complexes, namely 1-(carboxymethyl) pyridine-1-ium, 1-(2-carboxymethyl)-1-methylmorpholin-1-ium and 1-(2-carboxymethyl)-1-methylpyrrolidin-1-ium, which can capture the bromine in the



aqueous phase due to the addition of hydroxyl functional groups. Unfortunately, actual battery performances with these BCAs were not provided. Alternatively, a surface active agent (SAA), polyoxyethylene (20) sorbitan monolaurate (Polysorbate 20), was added to the electrolyte to enhance the mixing of the aqueous solution and polybromide complex phase (**Fig. 3b**), which improves the coulombic efficiency (CE) and ZBFB system stability [84]. Polarization tests showed that most  $\text{Br}_2/\text{Br}^-$  redox reactions occur at the electrode-aqueous phase interface, rather than the electrode-oily polybromide phase interface. Hence, a homogeneous aqueous catholyte is more favorable for the reduction reaction of bromine during the discharge process. Accordingly, the addition of Polysorbate 20 facilitated the mixing of catholytes and greatly improved the bromine reduction reactions, leading to enhanced CEs and cyclability.

Apart from bromine sequestration, modifications of the electrolyte composition and concentration can also enhance the ionic conductivity and  $\text{Br}_2/\text{Br}^-$  reaction kinetics. Kim and Jeon investigated different alternative supporting electrolytes, including lithium perchlorate ( $\text{LiClO}_4$ ), sodium perchlorate ( $\text{NaClO}_4$ ) and zeolite-Y, and found that the addition of zeolite-Y can improve the electrochemical stability of the ZBFBs compared to the commonly used  $\text{ZnCl}_2$  and  $\text{KCl}$  supporting electrolytes [85]. Wu et al. [86] employed  $\text{NH}_4\text{Cl}$  as a supporting electrolyte to enhance electrolyte conductivity, with which the EE of ZBFBs was improved from 60.4% to 74.3% at  $40 \text{ mA cm}^{-2}$ . In addition to salts, some acids have also been investigated as supporting electrolytes. For example, Adith et al. [87] found that the addition of 2 M

perchloric acid ( $\text{HClO}_4$ ) could improve the  $\text{Br}_2/\text{Br}^-$  redox kinetics and reduce the internal resistance of the system due to the improved ionic conductivity, leading to an enhanced VE of about 85% at the current density of  $30 \text{ mA cm}^{-2}$ . Methanesulfonic acid (MSA) also exhibits similar functions, which enables a ZBFB to achieve a high EE of 75% at  $40 \text{ mA cm}^{-2}$  [88]. Unfortunately, the presence of acid may trigger HER and accelerate the corrosion of Zn anode, which is detrimental to the ZBFBs.

#### 2.2.1.2 Membrane engineering

The commonly used membranes for ZBFBs can generally be divided into two categories, i.e., ion exchange membranes and porous separators. The former exhibits much lower bromine permeability and thus higher CEs, but the wide application is hindered by the high cost, while the latter features low cost, but the bromine crossover is more severe. However, because BCAs are typically used in ZBFBs and bromine usually exist in an oily phase, the CEs are acceptable and therefore porous separators are more widely used in ZBFBs. Nevertheless, to further promote the commercialization of ZBFBs, advanced membranes should be developed to inhibit bromine crossover and improve the battery performance [89].

To this end, commercial Daramic porous membrane was modified with pore filling agent, which was fabricated by dispersing multiwalled carbon nanotubes (MWCNT) as nanofiller into polyacrylonitrile (PAN) polymer matrix. The resulting MWCNT/PAN-Daramic composite membranes exhibited a dense morphology, which can effectively suppress bromine diffusion and increase the battery performance [90]. Similarly, a void-free membrane was prepared by impregnating Nafion into a porous

polypropylene (PP) separator, as illustrated in **Fig. 3c**. It was demonstrated that, although the Nafion/PP membrane exhibited a thickness of as low as 16  $\mu\text{m}$ , the  $\text{Br}_2$  permeability was two orders of magnitude lower than that of the 600- $\mu\text{m}$ -thick porous separator due to its dense morphology. Moreover, the composite membrane showed a lower specific area resistance, leading to an improved VE [91]. Furthermore, Hua et al. [92] developed a porous composite membrane with a separation layer, which was formed by introducing a complexing agent (MEPBr) into the porous Daramic separator (**Fig. 3d**). During the charging process, the generated bromine and polybromides can complex with the complexing agents and be captured in the separation layer, thus inhibiting bromine species crossover and reducing the self-discharge. Consequently, the ZBFB with the composite membrane delivered a high CE of 97.42% and an improved EE of 85.31% at 40  $\text{mA cm}^{-2}$  [92]. To address the trade-off between crossover and conductivity of ion exchange membrane, Han and Shanmugam proposed to introduce amphoteric functionalized silica ( $\text{Am-SiO}_2$ ) into the Nafion membrane. As displayed in **Fig. 3e**, the co-existence of positively and negatively charged functional groups can reduce the crossover of polybromide species through charging exclusion while balancing the bi-ionic transport abilities, thereby ensuring a high ionic conductivity. As a result, the ZBFB with this composite membrane can deliver a higher CE, VE, and EE compared to those with NRE-212 and SF600 membranes [93].

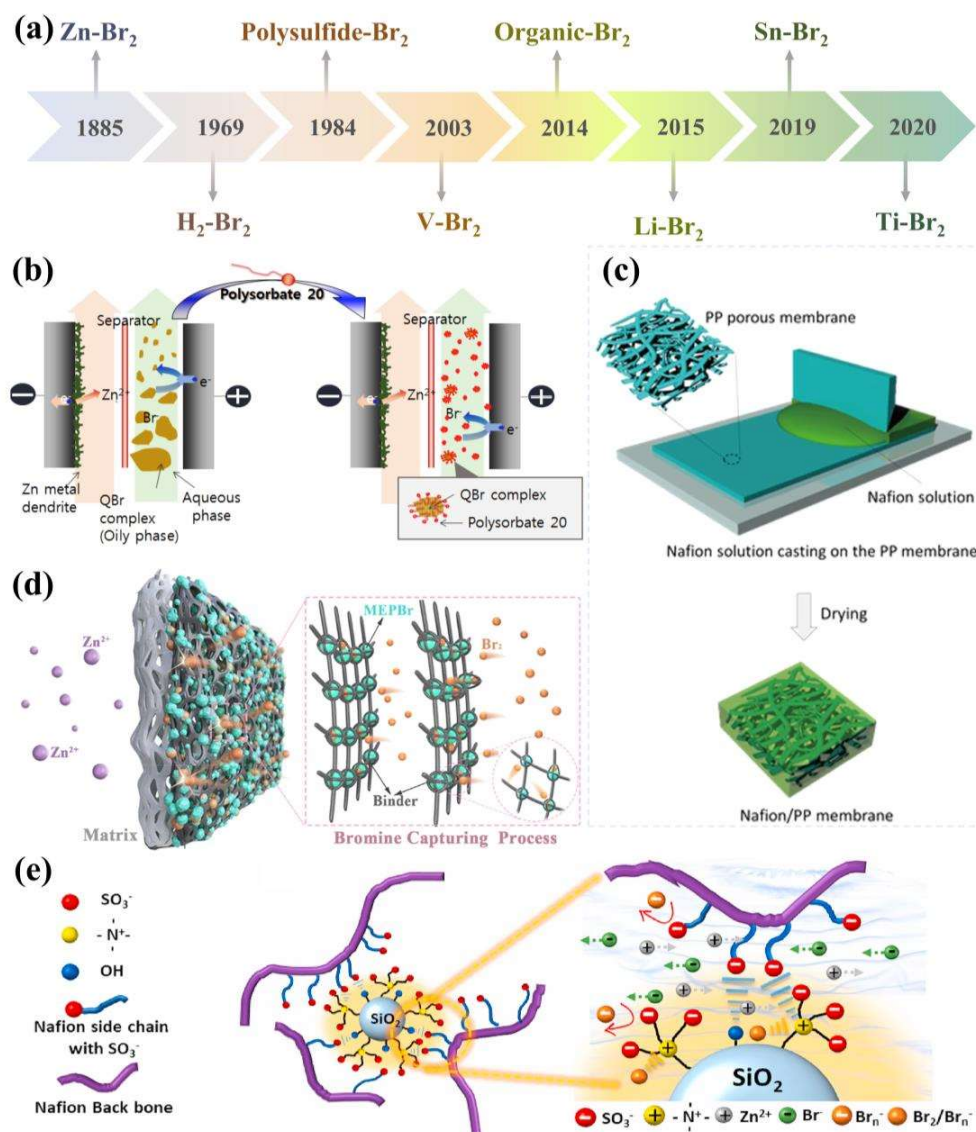


**Fig. 3.** (a) Timeline of the development of bromine-based flow batteries. (b) Schematic of the effect of Polysorbate 20 on improving the mixing of polybromide-complex and aqueous phases. Reproduced with permission from Ref. [84]. Copyright 2014, Elsevier. (c) Schematic of the Nafion/PP membrane fabrication process. Reproduced with permission from Ref. [91]. Copyright 2017, Springer Nature. (d) Bromine capture process of the MEPBr-Nafion-Daramic composite membrane. Reproduced with permission from Ref. [92]. Copyright 2021, Elsevier. (e)

Schematic illustration of the interaction between Nafion and Am-SiO<sub>2</sub> in the Nafion/Am-SiO<sub>2</sub> membrane. Reproduced with permission from Ref. [93]. Copyright 2022, Elsevier.

### 2.2.1.3 Electrode modifications

Electrode is a key component that largely determines the performance of ZBFBs as it not only provides active sites for electrochemical reactions but also pathways for mass/ion/electron transport. Because of their low cost, good electronic conductivity, high chemical and electrochemical stability, carbon materials are currently the most widely used cathode materials for ZBFBs [94,95]. At the early stage of ZBFBs, plastic-bonded-carbon by hot pressing the carbon black onto the polypropylene-based substrate was used as electrodes for Br<sub>2</sub>/Br<sup>-</sup> reactions [96]. These electrodes usually exhibit high surface area and activity but suffer from poor mechanical stability. The deterioration mechanism of the carbon plastic electrode was revealed by Futamata et al. [97]. They found that the formation of C-Br bond during electrochemical reactions would cause exfoliation and cracking on the electrode surface. Therefore, carbon felts (CFs) and graphite felts (GFs) with high mechanical strength are more promising alternative electrodes for ZBFBs. However, they provide low surface area and activity for Br<sub>2</sub>/Br<sup>-</sup> reactions. To overcome these challenges, different strategies have been developed. Zhang et al. [98] proposed a catalyst coated membrane (CCM) with high specific surface area to accelerate the Br<sub>2</sub>/Br<sup>-</sup> redox reactions. The CCM was placed between the separator and a CF, which greatly reduced the internal resistance due to the shortened ion transport distance between the activated carbon layer and membrane.

As a result, the CCM enabled the ZBFB to achieve an improved EE of 80.3% at 20 mA cm<sup>-2</sup>, in comparison to 73.2% when only conventional CF electrodes were used. Based on the CCM design, the same group investigated various carbon blacks as catalysts and found that Black Pearls 2000 (BP2000) exhibited the higher activity than the other three commercial carbons (i.e., acetylene black, expanded graphite, and CNT) toward Br<sub>2</sub>/Br<sup>-</sup> redox reactions [99]. To further boost the Br<sub>2</sub>/Br<sup>-</sup> reaction kinetics, they also designed and synthesized several advanced carbon materials. For example, a cage-like porous carbon (CPC) with a pore size of about 1.1 nm was fabricated (**Fig. 4a and b**). Density functional theory (DFT) calculations revealed that the Br<sup>-</sup> and MEP<sup>+</sup> have smaller diameters and can freely enter and exit the shell of the CPC. During the charging process, Br<sup>-</sup> ions are oxidized to Br<sub>2</sub>, which combines with the complexing agent in the cavity to form large-diameter bromine complexes and are trapped inside the shell, thus reducing Br<sub>2</sub> crossover. The combination of fast Br<sub>2</sub>/Br<sup>-</sup> reaction kinetics and bromine-capture capability of CPC allowed the ZBFB to achieve an ultrahigh CE of 98% and an EE of 81% at 80 mA cm<sup>-2</sup> [100]. Bimodal highly ordered mesostructure carbons (BOMCs) with large specific surface area and high activity for Br<sub>2</sub>/Br<sup>-</sup> redox couple were synthesized by an evaporation induced triconstituent co-assembly method. As shown in **Fig. 4c**, the highly ordered mesostructure can greatly reduce the mass transport resistance while the 2 nm pores on 5 nm pore walls facilitate Br<sub>2</sub> adsorption and provide more active sites for Br<sub>2</sub>/Br<sup>-</sup> reactions. As a consequence, the ZBFB assembled with BOMCs-based CCM was able to deliver an EE of 80.1% at the current density of 80 mA cm<sup>-2</sup> [101]. To promote the

1 application of advanced carbon materials, a facile and versatile way was proposed to  
2  
3 synthesize porous nano-sheet carbon (PNSC). After CO<sub>2</sub> activation, the PNSC  
4  
5 exhibited a highly porous loose structure, which not only enhances the ion diffusion  
6  
7 rate but also offers a high specific area of ca. 2085 m<sup>2</sup> g<sup>-1</sup>. When applied in ZBFBs,  
8  
9 the battery could deliver an improved EE of 82% at 80 mA cm<sup>-2</sup> [102].  
10  
11  
12  
13

14        Apart from the CCM design, the electrochemical performance of electrodes can  
15  
16 be enhanced by coating active materials on the fiber surface of GF or CF electrodes.  
17  
18 For example, Pt particles with high activity toward Br<sub>2</sub>/Br<sup>-</sup> reactions were deposited  
19  
20 on the GFs as an electrocatalyst through pulsed laser deposition (PLD) process. The  
21  
22 ZBFB assembled with this Pt coated electrode delivered a high EE of 88.02% at 50  
23  
24 mA cm<sup>-2</sup> [103]. It should be noted that although Pt exhibits a high catalytic activity,  
25  
26 the high cost would be a major obstacle for its application in aqueous flow cells,  
27  
28 which are aimed for large-scale energy storage. Munaiah et al. [104] studied the  
29  
30 catalytic activity of single wall carbon nanotubes (SWCNTs) with different purity  
31  
32 toward Br<sub>2</sub>/Br<sup>-</sup> reactions. It showed that higher purity SWCNTs exhibit better  
33  
34 electrochemical activity due to more available active sites. Consequently, the EE was  
35  
36 increased by 33% with the SWCNT modified electrode compared with pure CF  
37  
38 electrode. They also compared the electrochemical activity of SWCNTs and  
39  
40 MWCNTs for Br<sub>2</sub>/Br<sup>-</sup> reactions. It was found that SWCNTs exhibit higher activity  
41  
42 possibly due to a large amount of basal planes, while MWCNTs display better  
43  
44 reversibility based on peak separation in cyclic voltammograms (CV) [105].  
45  
46 Moreover, two dimensional nanomaterials, such as reduced graphene oxide (rGO)  
47  
48  
49  
50  
51  
52  
53  
54  
55  
56  
57  
58  
59  
60  
61  
62  
63  
64  
65

[106] and N-doped graphene nanoplatelets [107], have also been employed to improve the bromine kinetics in ZBFBs, with which the EEs of ZBFBs were greatly enhanced. However, the synthesis of these carbon materials requires sophisticated procedures, hindering their widespread applications. To circumvent this issue, Wu et al. [108] developed a simple yet effective approach to synthesize mesoporous carbon materials from biomass pomelo peel. Nickel salt was added in the precursor to simultaneously enhance the graphitization and create abundant mesopores on the carbon surface. Accordingly, the resulting carbon exhibited a remarkable electrocatalytic activity toward  $\text{Br}_2/\text{Br}^-$  redox reactions, thereby allowing the ZBFB to operate at a high current density of  $80 \text{ mA cm}^{-2}$  with an EE of 84.2%. In addition to high electrochemical activity for  $\text{Br}_2/\text{Br}^-$  redox reactions, some carbon materials with unique structures can also adsorb and capture bromine species, thereby inhibiting  $\text{Br}_2$  diffusion. As illustrated in **Fig. 4d**, the porous carbon nitride nanosheets (PCNS) with a large specific surface area provides abundant active sites for positive redox reactions, while the N-containing functional groups can absorb the generated  $\text{Br}_2$  and then confine bromine species in the PCNS interlayers. Consequently, the ZBFB installed with PCNS-modified electrode delivered a high CE and EE of 99.22% and 63.48% at a high current density of  $180 \text{ mA cm}^{-2}$  [109].

Direct surface treatment or modification of positive electrodes is another strategy to improve electrochemical activity. Suresh et al. [110] introduced oxygen functional groups onto the CF surface to increase the electrochemical activity and hydrophilicity through acid treatment. The ZBFB assembled with the modified electrode delivered



an improved VE of 86% at the current density of 20 mA cm<sup>-2</sup>. Moreover, the GF could be modified by thermal treatment and plasma treatment under oxygen and nitrogen atmospheres to simultaneously increase surface area and O- and N-containing functional groups. The ZBFB with the modified positive electrode showed an enhanced EE of 77% at 10 mA cm<sup>-2</sup> [111]. To further boost the surface area, cobalt-assisted thermal treatment was used to modify GF surface. The catalytic etching in the presence of Co resulted in aligned carbon nanostructures and abundant oxygen functional groups on the fiber surface, which can facilitate charge and mass transfer. Consequently, the EE of ZBFB was increased from 68% to 84% at 60 mA cm<sup>-2</sup> [112]. Furthermore, Lu et al. [113] proposed a multifunctional CF-based electrode (NTCF) with N-rich defects, which can enhance the absorption of bromine and facilitate the Br<sub>2</sub>/Br<sup>-</sup> reactions (**Fig. 4e**). Impressively, the NTCF enabled ZBFB to operate at a current density of as high as 180 mA cm<sup>-2</sup> with an EE of 63.07%. In addition, a composite electrode based on a CF supported TiN nanorod array with a 3D hierarchical structure (CTN) was proposed. Compared with the smooth surface of pristine CF (**Fig. 4f**), the nanorod array alignment and abundant pores in CTN (**Fig. 4g**) allow faster ion transfer and provide much more active sites for Br<sub>2</sub>/Br<sup>-</sup> redox reactions. Therefore, the ZBFB with this CTN electrode achieves an EE of 66% at an ultrahigh current density of 160 mA cm<sup>-2</sup> [114]. This work offers a new strategy for development of advanced electrodes for high-power density bromine-based flow batteries.

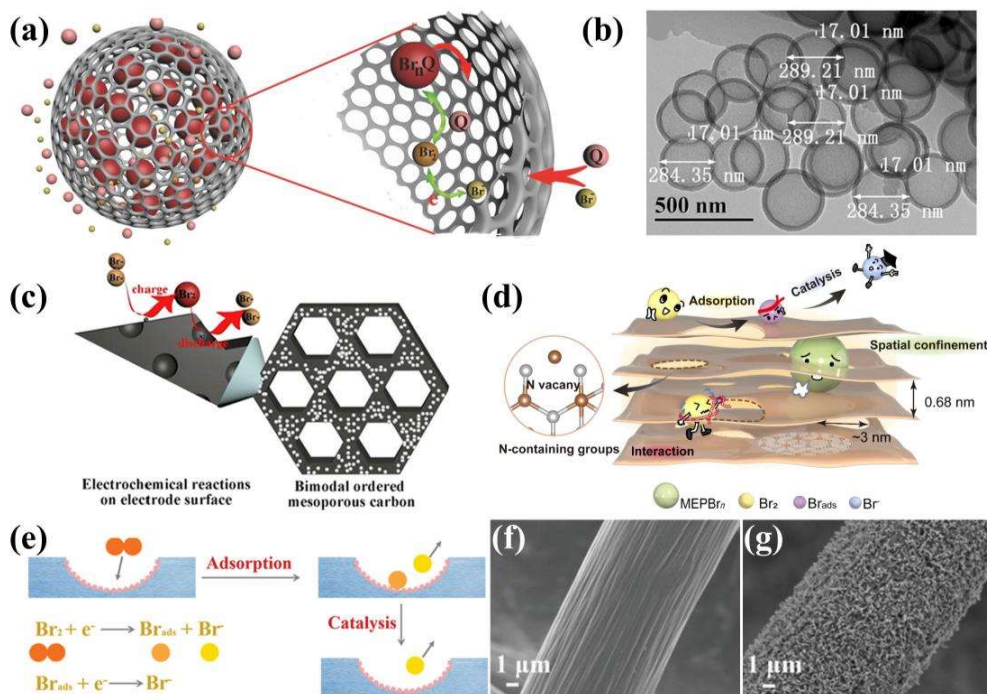


**Fig. 4.** (a) Working principle of cage-like porous carbon in bromine-based batteries; (b) TEM image of CPC. Reproduced with permission from Ref. [100]. Copyright 2017, Wiley-VCH. (c) Working principle of BOMCs applied in ZFBFs. Reproduced with permission from Ref. [101]. Copyright 2016, Elsevier. (d) Schematic diagram of adsorption and spatial confinement effects of PCNS. Reproduced with permission from Ref. [109]. Copyright 2022, Elsevier. (e) Reaction mechanism of  $\text{Br}_2/\text{Br}^-$  couple on NTCF. Reproduced with permission from Ref. [113]. Copyright 2021, Wiley-VCH. SEM images of (f) CF; and (g) CTN. Reproduced with permission from Ref. [114]. Copyright 2019, Wiley-VCH.

### 3.2.2 $\text{H}_2\text{-Br}_2$ regenerative fuel cells

Similar to  $\text{H}_2\text{-Cl}_2$  regenerative fuel cells,  $\text{H}_2\text{-Br}_2$  regenerative fuel cells have been developed as an alternative to  $\text{H}_2\text{-O}_2$  systems. Although the theoretical energy density of bromine-based cells is lower than that of their chlorine counterparts,  $\text{H}_2\text{-Br}_2$  cells

1 have higher power densities and lower voltage losses due to faster electrode kinetics  
2  
3 of  $\text{Br}_2/\text{Br}^-$  reactions and higher solubility of bromine in aqueous solutions [29]. The  
4  
5 research on  $\text{H}_2\text{-Br}_2$  fuel cell system was first conducted by Boyle and Glass in the late  
6  
7 1960s [115]. They not only reported the basic fuel cell structure of the  $\text{H}_2\text{-Br}_2$  system,  
8  
9 but also raised issues related to the cell construction, electrodes, electrolytes, and  
10  
11 membranes. Among them, electrode materials and crossover of bromine species  
12  
13 through the membrane were considered to be the main factors affecting the  
14  
15 performance of  $\text{H}_2\text{-Br}_2$  regenerative fuel cells [49,116]. Similar to the  $\text{H}_2\text{-Cl}_2$   
16  
17 regenerative fuel cells, bromine electrodes require highly active and  
18  
19 corrosion-resistant materials. At present, the research on bromine electrodes can be  
20  
21 basically divided into two categories: metal- and carbon-based electrodes.  
22  
23 Metal-based electrodes are mainly precious metals and their oxides. However, the  
24  
25 dense metal electrode surface leads to low porosity, poor catalyst dispersion, and  
26  
27 limited mass transfer of reactants. In addition, the use of noble metal electrodes also  
28  
29 increases the cost, which is not conducive to the commercialization of  $\text{H}_2\text{-Br}_2$   
30  
31 reversible fuel cells [117–119].  
32  
33  
34  
35  
36  
37  
38  
39  
40  
41  
42  
43  
44

45 Carbon materials are more widely used due to their low cost, high porosity, and  
46  
47 good chemical stability [120]. However, commercial carbon gas diffusion media that  
48  
49 are widely used as  $\text{Br}_2$  electrodes in  $\text{H}_2\text{-Br}_2$  fuel cells usually have low specific  
50  
51 surface area [121]. Therefore, modification of electrode materials is needed to  
52  
53 increase the surface area and accelerate the bromine reaction kinetics. To this end,  
54  
55 MWCNTs were directly grown on the electrode fiber surface via chemical vapor  
56  
57  
58  
59  
60  
61  
62  
63  
64  
65

deposition (CVD) method [121,122]. The MWCNT modified electrode exhibited 29 times higher surface area than the plain carbon electrode, enabling a H<sub>2</sub>-Br<sub>2</sub> flow cell to achieve a VE of 80%, which was 16% higher than that with three layers of plain carbon electrodes. To reduce the cost without compromising battery performance, carbon paper with one layer CNT was fabricated by the same group, which was estimated to cost 50% of the three-layer baseline carbon electrodes [123]. Moreover, commercial BP2000 carbon black with a large surface area (~1500 m<sup>2</sup> g<sup>-1</sup>) and high activity toward bromine redox reactions was used as catalyst for H<sub>2</sub>/Br<sub>2</sub> fuel cells. It was found that the GF/BP2000 composite electrode can greatly improve the cell performance, with which a peak power density of 1.28 W cm<sup>-2</sup> can be achieved [124]. In addition, acidic treatment of GF in a mixed solution of HNO<sub>3</sub> and H<sub>2</sub>SO<sub>4</sub> can also increase the specific surface area and electrocatalytic activity, which enabled 25% increase in power density compared to the original GF electrode [125].

Membranes also play a crucial role in determining the performance of regenerative H<sub>2</sub>-Br<sub>2</sub> fuel cells, particularly the CEs and stability. Yeo and McBreen investigated the transport properties (i.e., ionic conductivity, active species permeability and diffusivity) in a relatively stable Nafion membrane [52]. It was found that water content of membranes exhibits a significant effect on the transport properties. Moreover, because the bromine species are negatively charged, bromine migration in Nafion membrane is less than expected. Furthermore, Yeo and Chin explored the feasibility of H<sub>2</sub>-Br<sub>2</sub> cell for energy storage applications through theoretical and experimental analysis [126]. They found that the H<sub>2</sub>-Br<sub>2</sub> system can

1 achieve a high efficiency of 70% when the operating current density is less than 160  
2  
3 mA cm<sup>-2</sup>. Moreover, it was found that the electrolyte content of the membrane varies  
4  
5 considerably during cell operation, leading to a strong hysteresis effect on the cell  
6  
7 performance. Therefore, it was proposed to fill fuel cells with water or diluted HBr  
8  
9 acid solutions to avoid dehydration if the cell will be idle for a long period of time.  
10  
11 Lifetime studies by Barna and co-workers showed that H<sub>2</sub>-Br<sub>2</sub> fuel cells can run over  
12  
13 10000 h without significant degradation. However, the hydrophobic nature of anodes  
14  
15 and properties of the membrane are two parameters that largely determine the  
16  
17 operating lifetime of H<sub>2</sub>-Br<sub>2</sub> fuel cells [127]. Unfortunately, the corrosivity and  
18  
19 toxicity of Br<sub>2</sub> and HBr could not be completely solved, and the resulting increase in  
20  
21 system costs made the research of H<sub>2</sub>-Br<sub>2</sub> fuel cells interrupted for a time.  
22  
23  
24  
25  
26  
27  
28  
29

30  
31 After entering the 21<sup>st</sup> century, the study on H<sub>2</sub>-Br<sub>2</sub> fuel cells has become active  
32  
33 again due to the rapid development of renewable energies. In 2006, Livshits et al.  
34  
35 [128] reported a high-efficiency H<sub>2</sub>-Br<sub>2</sub> fuel cell based on a nanoporous  
36  
37 proton-conducting membrane (NP-PCM), which delivered a maximum power density  
38  
39 of 1.51 W cm<sup>-2</sup>, much higher than those of the hydrogen/air regenerative fuel cell  
40  
41 systems. Kreutzer et al. [129] evaluated the performance of a H<sub>2</sub>-Br<sub>2</sub> regenerative fuel  
42  
43 cell and compared it to that of H<sub>2</sub>-O<sub>2</sub> fuel cell. It was found the cell performance is  
44  
45 limited by the ohmic and mass transport resistance. Cho et al. [130] then investigated  
46  
47 the effect of electrolyte concentrations, membrane thickness, electrode and cell  
48  
49 configuration on the performance of H<sub>2</sub>-Br<sub>2</sub> flow batteries. They found that the HBr  
50  
51 concentration has a significant effect on the area-specific resistance (ASR) and thus  
52  
53  
54  
55  
56  
57  
58  
59  
60  
61  
62  
63  
64  
65

the cell performance. This finding led to the use of thin membranes, which dramatically enhanced the performance of H<sub>2</sub>-Br<sub>2</sub> flow batteries. The optimized cell was capable of delivering a peak power density of 1.46 W cm<sup>-2</sup> and a limiting current density of as high as 4 A cm<sup>-2</sup>. Tucker et al. [131] found that the performance of H<sub>2</sub>-Br<sub>2</sub> flow cells were largely determined by the membrane properties. In particular, a fundamental tradeoff was found between conductivity and crossover. Specifically, the system efficiency at high current densities is limited by the ionic conductivity while it is limited by crossover at low current densities. Membrane thickness, treatment procedure, and swelling state were found to be the three most important parameters that affect the battery performance and efficiency. It was demonstrated that the H<sub>2</sub>-Br<sub>2</sub> flow battery assembled with a NR212 (50 μm thick) membrane pretreated by immersing it in water at 70 °C showed the best performance. To further improve the performance of H<sub>2</sub>-Br<sub>2</sub> fuel cells while reducing costs, some researchers have made modifications to Nafion membranes to improve stability [132]. For example, Park et al. [133] proposed a Nafion/polyvinylidene fluoride (PVDF) nanofiber composite membrane (**Fig. 5a**). This composite Nafion/PVDF membrane has excellent bromine barrier properties, which leads to better performance of the H<sub>2</sub>-Br<sub>2</sub> fuel cell, although its ionic conductivity is lower than that of pristine Nafion 115 membrane. In order to further reduce the manufacturing cost of the membranes, the same group reported a simpler single-fiber Nafion/PVDF mat by electrospinning method. The PVDF simultaneously served as the role of electrospinning carrier polymer for Nafion, a mechanical reinforcement, and an uncharged component to suppress swelling. By

optimizing the composition, the composite membrane with a thickness of 18  $\mu\text{m}$  showed a low ASR and low bromine crossover. As a result, the  $\text{H}_2\text{-Br}_2$  flow cell equipped with the composite membrane delivered a peak power density of 1.31  $\text{W cm}^{-2}$ , outperforming that with Nafion 212 membrane (0.90  $\text{W cm}^{-2}$ ) [134,135]. Later, they fabricated another nanofiber composite membranes for regenerative  $\text{H}_2\text{-Br}_2$  fuel cells by electrospinning Nafion and polyphenylsulfone (PPSU) in a similar procedure [136]. Although the resulting composite membrane only showed slightly improved performance than Nafion 115 membrane in  $\text{H}_2\text{-Br}_2$  system, the content of perfluorosulfonic acid was greatly reduced, offering a cost advantage.

Eliminating the membrane is another approach to reducing cost. Braff et al. [137] first proposed a high-performance, low-cost, and membrane-less hydrogen bromine laminar flow battery. As illustrated in **Fig. 5b**, in the discharge mode, the HBr solution flows between the electrodes in the main channel to serve as the electrolyte. Meanwhile,  $\text{H}_2$  and the mixture of HBr and  $\text{Br}_2$  flow through their respective electrodes for electrochemical reactions. This unique membrane-less design enabled a power density of 0.795  $\text{W cm}^{-2}$  with a round-trip VE of 92% at 25% of peak power, which was almost equivalent to the performance of  $\text{H}_2\text{-Br}_2$  flow batteries with membranes. To unlock the potential of this type of battery, Alfisi et al. [138] performed detailed breakdown of resistance losses. It was shown that the main sources of loss result from the porous cathode, followed by the resistance of the electrolyte channel. Therefore, further research should be focused on these two aspects, such as employing the cathode with higher electrochemical activity and

1 reducing the electrolyte channel thickness. It should be noted that, although the  
2  
3 co-laminar flows allow the elimination of membrane, mass transport kinetics will be a  
4  
5 key issue when only diffusion and migration exist. Moreover, how to scale up the  
6  
7 membrane-less flow cells also remains a critical challenge, which requires more  
8  
9 innovative design.  
10  
11  
12

### 13 **3.2.3 Polysulfide-Br<sub>2</sub> flow batteries**

14  
15  
16 Polysulfide-Br<sub>2</sub> RFBs that use a sodium bromide aqueous electrolyte in the  
17  
18 cathode and a sodium polysulfide electrolyte in the anode was first reported by  
19  
20 Remick et al. about 40 years ago [139]. A cation-exchange membrane (CEM) is used  
21  
22 to separate the two half-cell solutions to prevent the direct reaction of bromine and  
23  
24 sulfide anions. Due to the difference in electrolyte concentration and charge/discharge  
25  
26 state, the open circuit voltage of this type of battery is generally 1.35-1.6 V and the  
27  
28 EE is around 60–65% with the operating temperature between 20 and 40 °C [140].  
29  
30 Because of the abundance and low cost of active materials, polysulfide-Br<sub>2</sub> RFBs  
31  
32 have once been regarded as a promising candidate for large-scale energy storage. For  
33  
34 example, Innogy Technology Ventures Limited developed an energy storage  
35  
36 technology based on polysulfide-Br<sub>2</sub> RFBs, which was known as the Regenesys  
37  
38 battery system in 2000 [141]. They tried to build a 20 MWh/15 MW utility-scale  
39  
40 storage plant for power arbitrage applications in the United Kingdom, which could  
41  
42 meet the electricity demand of 10000 households for a whole day. However, the  
43  
44 project was halted before completion in 2003 [142] mainly due to the efficiency loss  
45  
46 and safety risk about leakage of bromine-containing electrolyte.  
47  
48  
49  
50  
51  
52  
53  
54  
55  
56  
57  
58  
59  
60  
61  
62  
63  
64  
65



Although commercial demonstration of polysulfide-Br<sub>2</sub> RFBs has been attempted, research works on this technology were rarely reported. Zhao et al. [143] investigated the use of nickel foam and PAN-based CF as negative and positive electrodes for polysulfide-Br<sub>2</sub> RFBs, which enhanced the average EE to 77.2% at 40 mA cm<sup>-2</sup> in the initial 48 cycles. Cobalt has also been coated on CF as the negative electrode to boost the reaction kinetics of polysulfides, which lead to improved EE of >80% [144,145]. Scamman et al. [146,147] performed numerical modelling to predict the concentration variation and current distribution along the electrodes, as well as the battery performance of this system under different operating conditions. Results showed that the mass transport overpotential at the bromine electrode limits the performance during discharge process. Moreover, owing to self-discharge and electro-osmotic effects, significant performance drift occurs. Therefore, complex and rigorous electrolyte management is essential to ensure practical operation, which, however, significantly increases the cost. Additionally, polysulfide-Br<sub>2</sub> RFBs suffer from several other critical challenges, including severe crossover and sulfur deposition on the membrane. Therefore, this technology has not seen substantial progress for a long time and was gradually abandoned.

### 3.2.4 V-Br<sub>2</sub> flow batteries

The vanadium-bromine (V-Br<sub>2</sub>) flow battery was first proposed by Kazacos et al. [148] in 2003, aiming to improve the energy density and reduce the cost of VRFBs. However, this strategy also induces common issues associated with the Br<sub>2</sub>/Br<sup>-</sup> redox couple, including sluggish reaction kinetics, bromine corrosiveness and crossover.

Therefore, corresponding approaches have been adopted to address these challenges in V-Br<sub>2</sub> RFBs. Rui et al. [149] prepared few layered graphene oxide nanosheets with polymer binders (PVDF and SPEEK) as electrode materials to provide more active sites for Br<sub>2</sub>/Br<sup>-</sup> reactions due to the introduction of large number of oxygen-containing functional groups on the modified electrode surface. Similarly, functionalized SWCNTs with abundant oxygen-containing groups were found to be a promising catalyst for Br<sub>2</sub>/Br<sup>-</sup> redox couple compared with pristine graphite, MWCNTs and SWCNTs. The reasons are three folds. First, the oxygen-containing functional groups provide more reactive sites and reduce the charge transfer resistance for the Br<sub>3</sub><sup>-</sup>/Br<sup>-</sup> reaction. Second, the oxygen-containing groups are beneficial to the adsorption of Br<sup>-</sup>, thus accelerating the redox reaction. Third, the functional groups can improve the hydrophilicity of the electrode and reduce the contact resistance between the electrolyte and electrode [150].

To reduce the corrosiveness and crossover of bromine species that lead to severe self-discharge, BCAs were added into the electrolyte to inhibit the diffusion and volatilization of bromine. Apart from the tetrabutylammonium bromide and polyethylene glycol, Poon et al. [151] evaluated the effects of adding MEMBr and MEPBr to the electrolytes, which have been proved to be effective in reducing Br<sub>2</sub> vapors in ZBFBs. In addition, 1,2-dimethyl-3-ethylimidazolium bromide (DMEIm: C<sub>7</sub>H<sub>13</sub>BrN<sub>2</sub>) and 1,2-dimethyl-3-propylimidazolium bromide (DMPIIm: C<sub>8</sub>H<sub>15</sub>BrN<sub>2</sub>) can also be used as BCAs in V-Br<sub>2</sub> RFBs, which can not only capture the bromine species, but also increase capacities and EEs due to the improved reversible redox

1 reaction of  $V^{2+}/V^{3+}$  and diffusion coefficient of vanadium ions [152].

2  
3 Additionally, Vafiadi et al. [153] evaluated the performance of a variety of ion  
4 exchange membranes in the V-Br<sub>2</sub> RFBs and found that most of the ion exchange  
5 membranes were not suitable for this battery system due to the high resistance and  
6 low stability, except ABT3, Gore Select M04494 and Gore Select L01854. Further  
7 optimizations are needed to enhance the selectivity and ion exchange capacity of the  
8 membranes. The same group also discovered that the proprietary perfluorinated  
9 membrane VF02 pre-treated by V-Fuel delivered good chemical stability and low  
10 electrical resistance, showing promising applications for high-performance V-Br<sub>2</sub> flow  
11 batteries [154]. Winardi et al. [155] employed low-cost SPEEK membranes in the  
12 V-Br<sub>2</sub> flow battery for the first time in 2014. The SPEEK membranes can provide  
13 comparable performance to Nafion 117 (EE: 76% for SPEEK membrane and 75% for  
14 Nafion 117 membrane) in the presence of complexing agents (MEPBr and MEMBr)  
15 in the electrolyte. However, the SPEEK membrane suffers a greater degree of  
16 swelling, which may degrade their mechanical strength and battery performance.  
17 Therefore, more efforts are needed to design and synthesize membranes with high  
18 ionic conductivity, high selectivity, high stability and low cost to promote the  
19 development of V-Br<sub>2</sub> flow batteries.  
20  
21  
22  
23  
24  
25  
26  
27  
28  
29  
30  
31  
32  
33  
34  
35  
36  
37  
38  
39  
40  
41  
42  
43  
44  
45  
46  
47  
48

### 49 **3.2.5 Organic-Br<sub>2</sub> flow batteries**

50  
51 In search of negative redox couples to pair with bromine cathode, organic redox  
52 active species have attracted increasing attention [156]. The wide variety of organic  
53 compounds makes it easy to modify their chemical and electrochemical properties  
54  
55  
56  
57  
58  
59  
60  
61  
62  
63  
64  
65

through molecular engineering to meet the requirements of different applications [157]. Quinone derivatives are the most commonly used organics in aqueous bromine-based flow batteries due to the advantages of good electrochemical activity, reversibility, high solubility, and abundant resources in nature [158]. Huskinson et al. [159] first reported an aqueous organic-bromine flow battery using 9,10-anthraquinone-2,7-disulphonic acid (AQDS) as the negative active material. Remarkably, the AQDS-Br<sub>2</sub> flow battery achieved a peak galvanic power density exceeding 600 mW cm<sup>-2</sup> at the current density of 1300 mA cm<sup>-2</sup>. The same group further demonstrated that this battery could achieve good cycling performance, delivering an average discharge capacity retention of 99.84% per cycle and current efficiency of 98.35% after 750 deep cycles [160]. By optimizing the design and operating parameters, including operating temperature, electrolyte composition, flow rate, electrode and membrane materials and pre-treatment of these materials, the AQDS-Br<sub>2</sub> flow battery was able to deliver a power density of as high as 1.0 W cm<sup>-2</sup> [161].

However, there still exists some problems to be solved in quinone-Br<sub>2</sub> RFBs. For example, the open circuit voltage of this battery system is only about 0.8 V in acidic conditions, which greatly limits the energy density. To address this issue, anthraquinone derivatives with different structures (**Fig. 5c**) were designed and prepared as negative redox couples [162]. DFT calculations showed that the standard potential is closely related to the position and number of hydroxyl groups. Modifying the main chain of AQDS with more hydroxyl groups can increase the solubility and

cell voltage due to hydrogen bonding [159]. Experimental results showed that the standard redox potential of 1,8-dihydroxy-9,10-anthraquinone-2,7-disulphonic acid (DHAQDS) was 95 mV lower than AQDS, leading to 11% increase of the cell voltage [159]. Among the four evaluated anthraquinone derivatives, anthraquinone-2-sulfonic acid (AQS) is the most stable against bromine and reduction, allowing the AQS-Br<sub>2</sub> flow battery to deliver a higher open-circuit voltage and a higher peak galvanic power density than the initial AQDS-bromine system [162]. Interestingly, organic redox species show a strong dependence of pH, making it possible to increase the cell voltage by changing the pH. Khataee et al. [163] reported an AQDS-Br<sub>2</sub> flow battery with a high cell voltage of 1.3 V with different pH values at positive (~2) and negative (~8) sides, in comparison to 0.86 V when operated under acidic conditions on both sides. They further optimized the electrode thickness, flow rate, membrane thickness and concentration of active materials to reduce the resistance of the flow cell with differential pH, which led to a high power density of 0.45 W cm<sup>-2</sup> [164].

Viologen is another promising negative redox couple for bromine-based RFBs. Luo et al. [165] first reported a viologen-Br<sub>2</sub> flow battery by using an ammonium bromide (NH<sub>4</sub>Br) catholyte and a 1,10-bis(3-sulfonatopropyl)-4,4'-bipyridinium ((SPr)<sub>2</sub>V) anolyte, which displayed a high cell voltage of 1.51 V. Thanks to the high solubility of (SPr)<sub>2</sub>V and high cell voltage, the battery can achieve a high energy density of 30.4 Wh L<sup>-1</sup>. To further increase the solubility of viologen molecules, a hydrophilic and an electron-donating -OH group was introduced, forming (1,1')-di(2-ethanol)-4,4'-bipyridinium dibromide ((2HO-V)Br<sub>2</sub>) with an increased

solubility of  $> 2$  M. By pairing with a  $\text{Br}_2/\text{Br}^-$  positive redox couple, the battery achieved a high EE of 83.4% at a current density of  $40 \text{ mA cm}^{-2}$  and maintained stably run over 200 cycles [166]. Moreover, the viologen core structure can be modified with asymmetric functional groups such as propyl and triethyl ammonium propyl to increase the solubility and stability. As a result, the flow battery delivered a cell voltage of 1.66 V and excellent stability over 100 cycles with a high CE of 99% at  $40 \text{ mA cm}^{-2}$  [167]. However, the reduced state of viologen is unstable in the air and some types of viologen are toxic and hazardous to human health, which may hinder its application in large-scale energy storage.

### 3.2.6 Li- $\text{Br}_2$ flow batteries

Owing to the high theoretical capacity ( $3860 \text{ mAh g}^{-1}$ ) and lowest redox potential ( $-3.05 \text{ V vs. standard hydrogen electrode (SHE)}$ ), lithium (Li) metal has been widely regarded as a “holy grail” of batteries. Therefore, attempts have been made to pair a Li metal anode with  $\text{Br}_2/\text{Br}^-$  redox couple, forming various Li-Br batteries. Because of the high reactivity of Li metal, a  $\text{Li}^+$ -conducting solid electrolyte is required to separate the non-aqueous and aqueous electrolytes. Zhao et al. [168] first reported a static Li- $\text{Br}_2$  battery with a Li metal anode and a catholyte containing 1 M KBr and 0.3 M LiBr. This Li- $\text{Br}_2$  battery system showed excellent electrochemical performance, which delivered a high discharge potential of 3.9 V, a reversible capacity of  $290 \text{ mAh g}^{-1}$ , a specific power density of nearly  $1000 \text{ W kg}^{-1}$  and high capacity retention. To unlock the potential of this battery system, several Li-Br flow cells with innovative design have been developed [169–171]. For example, a

dual-mode rechargeable Li-Br<sub>2</sub>/O<sub>2</sub> fuel cell (**Fig. 5d**) was fabricated, which could fulfil multifunctional power requirements of autonomous underwater vehicles [170]. Specifically, the battery can operate in two modes: a low power mode with water and a high power mode with 1 M LiBr and 0.1 M Br<sub>2</sub> aqueous solution, with stable output voltages of 2 and 3 V for low and high mode operation, respectively. In 2016, Bai and Bazant [171] proposed a Li-Br<sub>2</sub> rechargeable fuel cell with a Li metal anode, a solid electrolyte LATP (Li<sub>2</sub>O-Al<sub>2</sub>O<sub>3</sub>-SiO<sub>2</sub>-TiO<sub>2</sub>-GeO<sub>2</sub>-P<sub>2</sub>O<sub>5</sub>) and a flat graphite electrode in highly concentrated bromine catholytes. To address the strong corrosion of bromine solution, a separate tank was used to store pure bromine and the battery system is illustrated in **Fig. 5e** and **f**. During charging process, liquid bromine is extracted and stored in a secondary tank, which can be released back to the primary electrolyte tank to maintain an optimum catholyte concentration. This unique battery design reduces energy loss due to evaporation and mitigates corrosion of LATP plates by maintaining a low bromine concentration. It was shown that the battery could discharge at a peak power density around 9 mW cm<sup>-2</sup> and deliver a theoretical specific energy of as high as 791.8 Wh kg<sup>-1</sup>. Although Li-Br<sub>2</sub> RFB can deliver an exceptional high cell voltage and energy density, the success of this battery strongly depends on the solid electrolytes, which are required to be highly ionic conductive, mechanically strong, and (electro)chemically stable. Unfortunately, current ceramic solid electrolytes are far from meeting these stringent requirements and thus, only proof-of-concept RFBs have been demonstrated. Moreover, safety is a great concern when the highly reactive Li metal that tends to form dendrite is coupled with an aqueous catholyte.

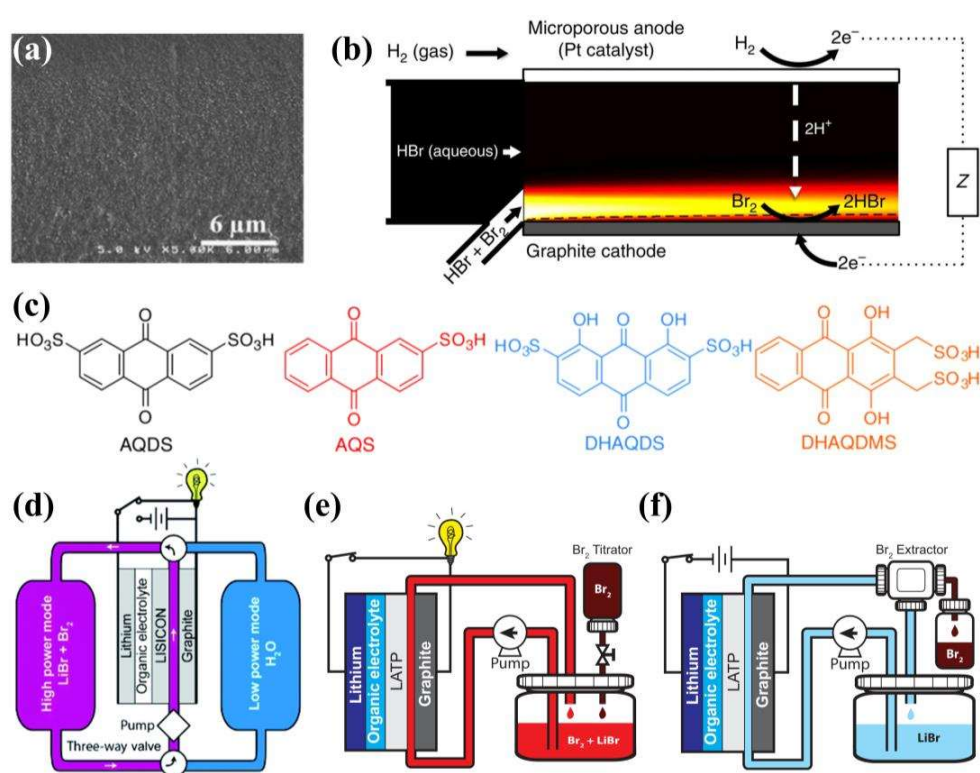


**Fig. 5.** (a) SEM image of the freeze-fractured cross section of a 55 vol% Nafion solution-cast blended membrane. Reproduced with permission from Ref. [133]. Copyright 2015, Elsevier. (b) Schematic of the membrane-less  $\text{H}_2\text{-Br}_2$  RFB. Reproduced with permission from Ref. [137]. Copyright 2013, Springer Nature. (c) Molecular structures of AQDS, AQS, DHAQDS and DHAQDMS. Reproduced with permission from Ref. [162]. Copyright 2016, Wiley-VCH. (d) Schematic demonstration of the dual-mode operation of the fuel cell. Reproduced with permission from Ref. [170]. Copyright 2015, Royal Society of Chemistry. (e) Discharging mode with a  $\text{Br}_2$  titration system; (f) Regenerative mode with a  $\text{Br}_2$  extractor in a  $\text{Li-Br}_2$  flow cell. Reproduced with permission from Ref. [171]. Copyright 2016, Elsevier.



### 3.2.7 Sn-Br<sub>2</sub> flow batteries

A novel Sn-Br<sub>2</sub> redox flow battery was developed by Zeng et al. [172] in 2019, which showed a high operating current density, long cycle life, and low cost. The battery system adopted Br<sub>2</sub>/Br<sup>-</sup> as the positive redox couple and Sn<sup>2+</sup>/Sn as the negative couple, which can deliver a working voltage of about 1.2 V. During discharge process, metallic Sn at the negative electrode loses electrons and is oxidized to Sn<sup>2+</sup>, while the Br<sub>2</sub> at the positive electrode is reduced to Br<sup>-</sup>. The process is reversed when being charged. This Sn-Br<sub>2</sub> flow battery can deliver a CE of 97.6% and EE of 82.6% at the high current density of 200 mA cm<sup>-2</sup>. More importantly, a Sn reverse-electrodeposition method could be employed to solve the cross-contamination problem of Sn ions and in-situ recover the capacity, which greatly improves the cycle life. Moreover, they estimated the capital cost of Sn-Br<sub>2</sub> flow battery can be reduced to \$148 kWh<sup>-1</sup> at the optimistic scenario, which is promising for large-scale energy storage.

### 3.2.8 Ti-Br flow batteries

Recently, a low-cost and long-life titanium-bromine flow battery (TBFB) consisting of HBr and Ti(SO<sub>4</sub>)<sub>2</sub> as positive and negative active materials was proposed by Li et al. [173] for large-scale energy storage. HCl was used as the supporting electrolyte to improve ionic conductivity and suppress the formation of HBrO. Moreover, a novel complexing agent (i.e., 3-chloro-2-hydroxypropyltrimethyl ammonium chloride (CHA)) was adopted to sequester bromine and reduce Br<sub>2</sub> diffusion. Unlike conventional complexing agents (e.g., MEPBr and MEMBr) that

capture bromine into a separate oily phase, the CHA-Br<sub>n</sub> complex maintains a nearly homogeneous phase because of the hydrophilic hydroxyl groups, which is beneficial to the operation of RFBs. CV test results show that there is no significant change in the electrochemical process after the addition of the CHA complexing agent. The complexation mechanism between CHA and polybromides was investigated by Raman spectroscopy combined with DFT calculations. It was found that at low state of charge (SOC), the charging products are mainly CHABr<sub>3</sub>, and as the SOC increases, CHABr<sub>3</sub> further complex with the generated Br<sub>2</sub> to produce CHABr<sub>5</sub>. It was demonstrated that the TBFB can deliver an EE of more than 80% at a current density of 40 mA cm<sup>-2</sup> and operate continuously for more than 1000 cycles without obvious performance degradation, superior to other deposition-dissolution type flow batteries that may suffer from dendrite growth and areal capacity limitation. More impressively, a 300 W TBFB stack was constructed and tested, which could stably run for more than 500 cycles, showing a good prospect for large-scale energy storage applications.

To further increase the energy density, the same group proposed a novel Br<sup>+</sup>/Br<sup>-</sup> redox couple by intercalating Br<sup>+</sup> into graphite to form a bromine-graphite intercalation compound in strongly acidic electrolytes. This new redox couple not only involved two electron transfer but also exhibited a 0.5 V higher redox potential compared to Br<sub>2</sub>/Br<sup>-</sup> reaction. Consequently, the TBFB with Ti(SO<sub>4</sub>)<sub>2</sub> as the anolyte could deliver a 65% higher energy density. Moreover, the battery can be operated at a current density of 30 mA cm<sup>-2</sup> with an EE of 80% and cycled for over 300 cycles. However, it should be noted that the capacity of this type of flow battery will be

1 determined by the intercalation sites in graphite, which differs considerably from  
2  
3 conventional bromine-based flow batteries. Furthermore, repeated insertion and  
4  
5 extraction of bromine into/out of graphite might damage the structure, leading to  
6  
7 capacity decay [174].  
8  
9

10  
11 To sum up, bromine-based flow batteries have attracted considerable research  
12  
13 interests over the past decades with various systems been proposed. However, the  
14  
15 commercialization of bromine-based RFBs still has a long way to go due to many  
16  
17 technical bottlenecks. One of the most critical challenges is the safety issue as  
18  
19 bromine is volatile, highly reactive and toxic. Luckily, unlike chlorine, these issues  
20  
21 can be effectively addressed by adding BCAs, making it more practical for real-world  
22  
23 applications. ZBFBs are one of the successful examples to demonstrate the  
24  
25 effectiveness of BCAs. Nevertheless, it should be noted that the addition of BCAs  
26  
27 only greatly reduces the vapor pressure of bromine, not eliminating it. Moreover, the  
28  
29 commonly used BCAs will lead to the formation of a separate oily phase, which not  
30  
31 only complicates the system design but also decreases the energy efficiency due to the  
32  
33 poor mixing of the two phases. Therefore, it is desired to develop new BCAs that can  
34  
35 strongly capture bromine in the aqueous phase without affecting the electrochemical  
36  
37 kinetics. Systems that can quickly and accurately detect the leakage of bromine will  
38  
39 also be needed to address the safety issues of bromine-based flow batteries.  
40  
41 Concurrently, more efforts should be devoted to developing advanced electrode and  
42  
43 membrane materials to tackle the challenges of sluggish reaction kinetics and bromine  
44  
45 crossover. Moreover, although various redox couples have been reported to pair with  
46  
47  
48  
49  
50  
51  
52  
53  
54  
55  
56  
57  
58  
59  
60  
61  
62  
63  
64  
65

the bromine electrodes, most of them suffer from certain disadvantages. Hence, future research should also focus on the development of new negative redox active species, in order to create new-generation bromine-based flow batteries that can offer high energy density, high energy efficiency, long cycle life and low cost.

### 3.3 Iodine-based flow batteries

Compared with bromine, iodine is less corrosive and exhibits a high solubility in aqueous solution when complexed with halide ions. Moreover, there are less environmental problems caused by volatilization of active materials [175]. Therefore, aqueous iodine-based flow batteries have received increasing attention in the past decade.

#### 3.3.1 Polysulfide-I<sub>2</sub> flow batteries

Polysulfide is one of the promising anolytes to pair with iodine catholyte due to its high solubility, low cost, and resource abundance. Li et al. [176] reported a polysulfide-I<sub>2</sub> flow battery (PSIFB) with GF as the positive electrode and nickel foam as the negative electrode. It was demonstrated that both S<sub>2</sub><sup>2-</sup>/S<sup>2-</sup> and I<sub>3</sub><sup>-</sup>/I<sup>-</sup> redox couples exhibit superior electrochemical reversibility and the PSIFB can achieve a high energy density of 43.1 Wh L<sup>-1</sup> based on both anolyte and catholyte. Moreover, it was estimated that the material cost of PSIFB could be only \$85.4 kWh<sup>-1</sup>, much lower than that of VRFBs [177]. Later, Su et al. [178] also reported a PSIFB with Na<sup>+</sup> as the working ion to balance the charge in the electrolytes. The optimized battery delivered a peak power of 65 mW cm<sup>-2</sup> and stable cycling performance for over 200 cycles at a current density of 20 mA cm<sup>-2</sup>. However, the power density and EE of this type of

battery are limited by the sluggish reaction kinetics. To address this issue, various catalysts have been developed to improve the battery performance. Ma et al. [179] developed nanostructured CoS<sub>2</sub>/CoS heterojunction electrocatalyst with uneven charge distribution for both I<sub>3</sub><sup>-</sup>/I<sup>-</sup> and S<sub>x</sub><sup>2-</sup>/S<sup>2-</sup> reactions. This catalyst can improve the absorptivity of charged ions and promote charge transfer, thus boosting the reaction kinetics. As a result, catalyst modified GF electrode enabled the PSIFB to achieve a high EE of 84.5% at a current density of 10 mA cm<sup>-2</sup> and a power density of 86.2 mW cm<sup>-2</sup>. Qin et al. [180] synthesized Cu<sub>7</sub>S<sub>4</sub>/CNT composites (**Fig. 6a**) as a bifunctional catalyst for PSIFBs. It was confirmed by electrochemical performance tests and DFT simulations that the Cu<sub>7</sub>S<sub>4</sub>/CNT composites could effectively adsorb polysulfides and polyiodides and improve their reaction kinetics. The PSIFB with the Cu<sub>7</sub>S<sub>4</sub>/CNT catalyst could deliver a peak power density of 84.6 mW cm<sup>-2</sup>, in comparison to ~6.5 mW cm<sup>-2</sup> for the battery with bare CNT electrode. Moreover, the flow battery can stably run for over 500 h at 30 mA cm<sup>-2</sup> without detectable efficiency degradation. Recently, Liu et al. [181] synthesized a bifunctional NiCo<sub>2</sub>S<sub>4</sub> nanoarray on carbon paper electrode (**Fig. 6b**) to improve the redox kinetics of both polysulfides and polyiodides, which allowed PSIFB to deliver a peak power density of 82.4 mW cm<sup>-2</sup> at 160 mA cm<sup>-2</sup> and demonstrate excellent cycle stability with a capacity decay rate of 0.218% per day for 3400 h.

Apart from synthesis of catalysts, novel magnetic flowable electrodes (MFE) were developed to improve the performance of PSIFBs, as shown in **Fig. 6c** [182]. To prepare the MFE, the magnetically modified CNTs were dispersed in the electrolyte,

and then permanent neodymium magnets were embedded behind the current collector to let the magnetic field pass through the flow battery channels. Under the action of flowing electrolyte, the magnetic CNTs were aggregated onto the graphite bipolar plate to form well-structured nanoscale osmotic networks and chains, which served as the positive electrode. Impressively, even with small amounts of magnetic CNTs in the electrolyte, the MFE can achieve large electrochemical active surface area and porosity, which reduces cell impedance and pump losses. Accordingly, the PSIFB with a MFE can achieve a high EE of 79.3% at 20 mA cm<sup>-2</sup> and stably run for over 200 cycles, outperforming most reported iodine-based RFB systems. The same group also dispersed hydrophilic magnetic MWCNTs (modified MWCNTs with iron oxide nanoparticles) in positive electrolyte to prepare a stable magnetic nanofluidic electrolyte. Reductions in ohmic resistance as well as charge-transfer and mass-transfer resistances of the magnetic nanofluid electrolyte were observed compared to the case without magnetic MWCNTs. The resulting PSIFB delivered enhanced performance with a high CE of nearly 100% and an EE of 79.91% at 20 mA cm<sup>-2</sup>. In addition to improving battery performance, MMWCNTs can be separated and recovered using magnetic decantation during electrolyte replacement in redox flow batteries, thus retaining system cost-effectiveness. Although the battery stability under longer continuous operation needs to be improved, the innovative concept of applying MMWCNTs to the optimization of electrodes and electrolytes provides new opportunities for the development of next-generation high-performance, low-cost flow batteries [183].

It should be noted that because the active species in negative and positive electrolytes are different in PSIFBs, crossover is a critical challenge for this type of battery. The crossover of active species will not only result in a low CE but also generate insulating and insoluble products (i.e., sulfur and iodine) in the electrode and/or membrane, which will degrade the battery performance. More importantly, the pH of negolyte (alkaline) and posolyte (weakly acidic) are different and the diffusion of OH<sup>-</sup> from negolyte to posolyte will be detrimental to the reversibility and stability of I<sub>3</sub><sup>-</sup>/I<sup>-</sup> redox couple. To overcome these challenges, Li and Lu [184] designed a charge-reinforced ion-selective (CRIS) membrane to absorb the polysulfide and polyiodide anions on the negative and positive side of membrane, respectively. Specifically, polyvinylidene fluoride (PVDF) bonded Ketjen black carbon (KB) was infiltrated into the Nafion membrane. The PVDF with high hydrophobicity can reduce water uptake and mitigate swelling while KB with high surface area can absorb and accumulate the negatively charged polysulfide/polyiodide anions, which can electrostatically repel the active species and thus reduce the crossover, as illustrated in **Fig. 6d**. Moreover, KB with high electrical conductivity will also promote the full conversion of the electrochemical reactions in both electrodes. As a result, the PSIFB with CRIS membrane can be stably cycled for over 500 cycles (3.1 months) at 17.9 Ah L<sup>-1</sup>. In addition, techno-economic analysis showed that the CRIS-enabled PSIFBs could offer a low levelized cost of storage, which is promising for long-duration energy storage. This work provides a new direction for the development of highly-selective ion-exchange membranes, and this approach may be applied in other

polychalcogenides and polyhalide-based RFBs [184].

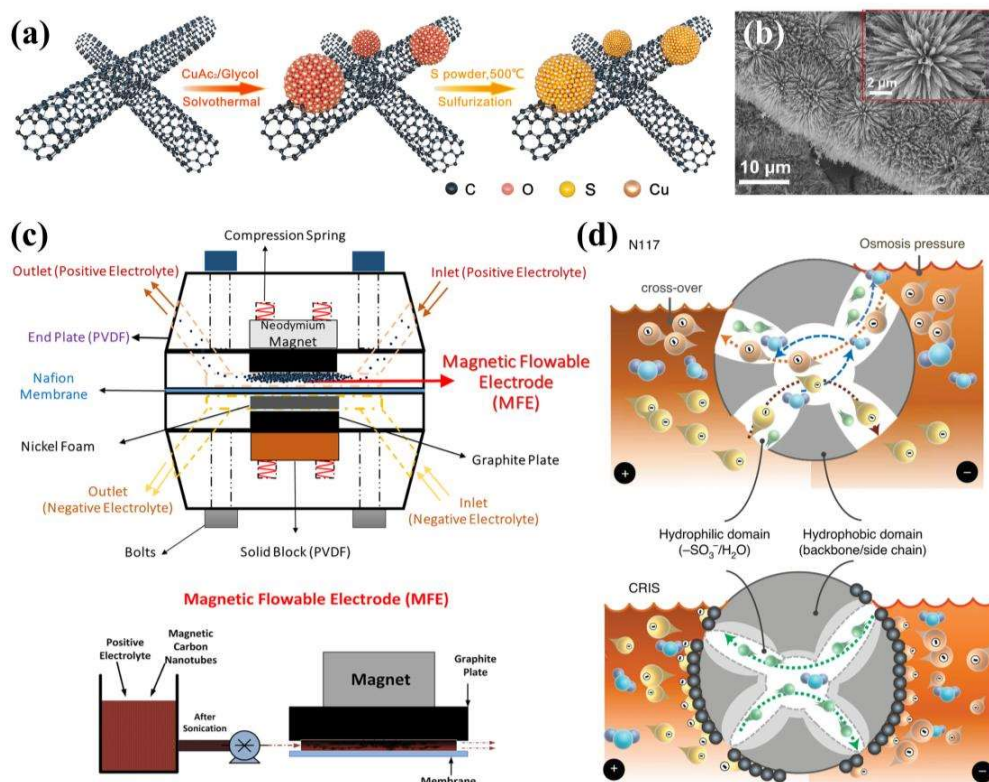


**Fig. 6.** (a) Scheme for the Cu<sub>7</sub>S<sub>4</sub>/CNT synthetic process. Reproduced with permission from Ref. [180]. Copyright 2021, Elsevier. (b) SEM images of NiCo<sub>2</sub>S<sub>4</sub> nanoarray on carbon paper. Reproduced with permission from Ref. [181]. Copyright 2022, Elsevier. (c) Schematic illustration of the PSIFB with an MFE on the positive side. Reproduced with permission from Ref. [182]. Copyright 2021, American Chemical Society. (d) Comparison between the pristine Nafion-117 membrane and CRIS membrane in polysulfide-I<sub>2</sub> RFBs. Reproduced with permission from Ref. [184]. Copyright 2021, Springer Nature.

### 3.3.2 Zn-I<sub>2</sub> flow batteries

Due to the superiority of iodine to its bromine counterpart, the iodine/iodide positive redox couple has been proposed to replace bromine in ZBFBs to develop



zinc-iodine flow batteries (ZIFBs). The performances of ZIFBs are summarized and compared in **Table S2**. Li et al. [185] first reported the ZIFB in 2015, using a near-neutral 5.0 M  $\text{ZnI}_2$  electrolyte for both cathode and anode, which was separated by a Nafion 115 membrane. The ZIFB exhibited an open circuit voltage of about 1.3 V and a discharge energy density of  $167 \text{ Wh L}^{-1}$ , which is nearly seven times higher than the current aqueous VRFBs and close to the lower limit of energy density of  $\text{LiFePO}_4$  cathode-based lithium-ion batteries. However, the EE of ZIFBs is low even at small current densities, which may be due to the poor reversibility and reaction kinetics of  $\text{I}_3^-/\text{I}^-$  redox couple. Accordingly, nanoporous metal-organic frameworks (MOFs), i.e.,  $\text{Ti}_8\text{O}_8(\text{OH})_4[(\text{O}_2\text{C}-\text{C}_6\text{H}_5-\text{CO}_2)]_6$  (MIL-125- $\text{NH}_2$ ) and  $\text{Zr}_6\text{O}_4(\text{OH})_4[\text{O}_2\text{C}-\text{C}_6\text{H}_2(\text{CH}_3)_2-\text{CO}_2]_6$  (UiO-66- $\text{CH}_3$ ), with high surface area were exploited as electrocatalysts to accelerate the  $\text{I}_3^-/\text{I}^-$  redox reactions. As shown in **Fig. 7a** and **b**, both catalyst particles are coated uniformly on the surface of GFs. At a current density of  $30 \text{ mA cm}^{-2}$ , MIL-125- $\text{NH}_2$  and UiO-66- $\text{CH}_3$  modified electrodes could enable 6.4% and 2.7% increase in EE but the latter is more stable in the weakly acidic electrolyte [186]. In addition to the reaction kinetics, the deposition of insulating  $\text{I}_2$  film (**Fig. 7c**) on electrode surface due to the slow conversion reaction of  $\text{I}_2$  to  $\text{I}_3^-$  ions may impede the further oxidation of  $\text{I}^-$  ions and limit the operating current density [187]. In order to reduce or eliminate the negative impact of the  $\text{I}_2$  film on battery performance, Zhao et al. [188] proposed to add organic solvents as a cosolvent to better solvate  $\text{I}_2$  and found that acetonitrile (ACN) can considerably accelerate the dissolution kinetics of  $\text{I}_2$ . DFT calculations revealed that the addition of cosolvent

could weaken the interaction of iodine with the carbon electrode surface. Accordingly, the addition of ACN enabled the ZIFB to operate at a high current density of 100 mA cm<sup>-2</sup> for over 170 cycles. Yang et al. [189] found that polyvinylpyrrolidone (PVP) could complex with iodine to form soluble PVP-2I<sub>3</sub><sup>-</sup>, which avoids the precipitation of I<sub>2</sub> and greatly promotes the oxidation of I<sup>-</sup> to I<sub>3</sub><sup>-</sup>. The absence of I<sub>2</sub> film could improve the electrode conductivity and thus lead to a high EE of 78% at 20 mA cm<sup>-2</sup>. Even with a high KI concentration of 6 M, the ZIFB can still deliver an EE of 70% and long-term cycling stability for over 600 cycles.

Membranes with high selectivity and conductivity are essential to improve the performance of ZIFBs. To this end, MOFs selective layers, UiO-66/-67 (C<sub>48</sub>H<sub>28</sub>O<sub>32</sub>Zr<sub>6</sub>/C<sub>84</sub>H<sub>52</sub>O<sub>32</sub>Zr<sub>6</sub>), were coated on Daramic porous substrates to form a defect-free composite membrane via a binder-controlled restrained second-growth method (BRSM) as illustrated in **Fig. 7d**. The ZrO<sub>2</sub> seeds were first introduced onto the Daramic membrane with binders, which gradually dissolved and left space for MOFs growth in the subsequent solvothermal process. Meanwhile, Zr<sup>4+</sup> slowly released from ZrO<sub>2</sub> seeds and in situ grew to a UiO-66/67 layer on the substrate, forming the defect-free MOF composite membrane. Thanks to the well-ordered pores of MOFs, the resulting membrane displayed an excellent selectivity of K<sup>+</sup> and reduced the active species crossover. Consequently, the CE of ZIFB was enhanced from 88.4% to 94.5% at 80 mA cm<sup>-2</sup> [190]. In addition, the uniform pore size of the MOF-modified membrane facilitated homogenous zinc fluxes, which led to more even Zn deposition and greatly suppressed the dendrite growth. Gao et al. [191]

1 synthesized a cost-effective host-guest-based membrane by incorporating starch into  
2  
3 the chitosan matrix to impede polyiodide crossover. The “guest” polyiodide can be  
4  
5 arranged in the inner cavity of starch and form complexes with starch and chitosan  
6  
7 due to the strong interaction between host and guest molecules. This bio-derived  
8  
9 membrane enabled the ZIFB to deliver a CE of 98.6% at 80 mA cm<sup>-2</sup> and stably run  
10  
11 for over 200 cycles without apparent efficiency decay. Interestingly, Xie et al. [192]  
12  
13 reported that a ZIFB could self-recover from micro-short-circuiting by employing a  
14  
15 porous polyolefin membrane as the I<sub>3</sub><sup>-</sup> adsorbed in the membrane pores could react  
16  
17 with Zn dendrites (**Fig. 7e**). Together with the high ionic conductivity, the ZIFB could  
18  
19 operate at 80 mA cm<sup>-2</sup> for over 1000 cycles (3 months). More remarkably, the 700 W  
20  
21 stack could stably run over 300 cycles at 80 mA cm<sup>-2</sup>, showing great promise for  
22  
23 practical application.  
24  
25  
26  
27  
28  
29  
30  
31  
32

33 In most iodine-based RFBs with I<sub>3</sub><sup>-</sup>/I<sup>-</sup> redox couple, only two-thirds of the iodide  
34  
35 species are involved in the redox reaction while the remaining iodide ions act as a  
36  
37 complexing agent to stabilize the I<sub>2</sub> by forming high soluble I<sub>3</sub><sup>-</sup> (I<sub>2</sub>I<sup>-</sup>) (**Fig. 7f**), which  
38  
39 greatly reduces the utilization of the iodine element and limits the energy density of  
40  
41 the RFBs. To unlock the capacity of iodide species, Weng et al. [193] added Br<sup>-</sup> to the  
42  
43 catholyte to complex I<sub>2</sub> to form stable I<sub>2</sub>Br<sup>-</sup>. The oxidation of Br<sup>-</sup> was avoided by  
44  
45 setting a suitable cut-off voltage. Accordingly, the zinc/iodine-bromide battery  
46  
47 demonstrated a significantly improved energy density of 101 Wh L<sup>-1</sup>. Moreover, this  
48  
49 strategy can also be applied to a nonaqueous lithium/iodine-bromide battery,  
50  
51 providing a new direction to develop high-energy-density halogen-based energy  
52  
53  
54  
55  
56  
57  
58  
59  
60  
61  
62  
63  
64  
65

storage systems. Jian et al. [194] also reported that the  $\text{Br}^-$  ions of  $\text{NH}_4\text{Br}$  supporting electrolyte can unlock the capacity of iodine. In addition, the addition of  $\text{NH}_4\text{Br}$  can enhance the ionic conductivity and suppress Zn dendrite formation, thereby leading to a higher energy density, higher EE, and longer cycle life for ZIFBs. Similarly, a  $\text{NH}_4\text{Cl}$  supporting electrolyte was reported to boost the capacity and performance of ZIFBs. It was demonstrated that the  $\text{NH}_4\text{Cl}$  supported ZIFB achieved a high energy density of  $137 \text{ Wh L}^{-1}$ , a CE of  $\sim 99\%$ , an EE of  $\sim 80\%$ , and a cycle-life of 2500 cycles due to the contribution of both  $\text{NH}_4^+$  and  $\text{Cl}^-$  ions [195]. To further increase the energy density of ZIFBs, the same group proposed to replace the acidic anolyte with an alkaline solution. It was demonstrated that the hybrid alkaline ZIFB exhibited an operative voltage of 0.47 V higher than that of conventional ZIFB, which eventually led to an unprecedented energy density of  $330.5 \text{ Wh L}^{-1}$ . Although promising, the use of alkaline Zn anode and electrolytes with different pH values will bring several critical challenges, including severe Zn dendrite formation, Zn corrosion, electrolyte crossover, which greatly sacrifice the battery performance. In fact, the reported battery can only run for 70 cycles at  $10 \text{ mA cm}^{-2}$  [196].

Another strategy to achieve high energy density of ZIFB is to adopt the single flow configuration and take advantage of the formation and precipitation of  $\text{I}_2$ . Xie et al. [197] developed a zinc-iodine single flow battery (ZISFB) using a non-flowing high-concentration electrolyte (7.5 M KI and 3.75 M  $\text{ZnBr}_2$ ) at the positive electrode. Due to the avoidance of electrolyte circulation,  $\text{I}^-$  ions in the positive electrolyte can be fully charged to solid  $\text{I}_2$  and deposited within the 3D porous CF electrode, thereby

1 leading to a high energy density of 205 Wh L<sup>-1</sup>, which is approaching the theoretical  
2  
3 value (240 Wh L<sup>-1</sup>). More importantly, the single flow battery could deliver a CE of  
4  
5 97% and an EE of 81% at 40 mA cm<sup>-2</sup> as well as a longer cycle life of more than 500  
6  
7 cycles [197]. Ito et al. [198] found that propylene carbonate (PC) can complex with I<sub>2</sub>  
8  
9 to form a hydrophobic polyiodide complex due to the large dipole moment between  
10  
11 PC and I<sub>2</sub>. The PC/I<sub>2</sub> complex can accelerate the I<sub>2</sub> dissolution rate on the cathode and  
12  
13 sinks to the bottom of the electrolytic cell under gravity, thus preventing the crossover  
14  
15 of polyiodides in the aqueous electrolyte even without the presence of CEM.  
16  
17 Consequently, the addition of PC enabled the ZISFB to achieve a high CE of over  
18  
19 90% without CEM. However, only 1.5 M NaI was used as active species and the  
20  
21 corresponding discharge charge capacity was 22.7 Ah L<sup>-1</sup>. In principle, if the  
22  
23 generated I<sub>2</sub> can be captured into a second phase and release back during discharge  
24  
25 process as demonstrated in this work, it is possible to design an iodine-based flow  
26  
27 battery with high energy density, which requires much more efforts in  
28  
29 designing/selecting more suitable complexing agents.  
30  
31  
32  
33  
34  
35  
36  
37  
38  
39  
40  
41  
42  
43  
44  
45  
46  
47  
48  
49  
50  
51  
52  
53  
54  
55  
56  
57  
58  
59  
60  
61  
62  
63  
64  
65

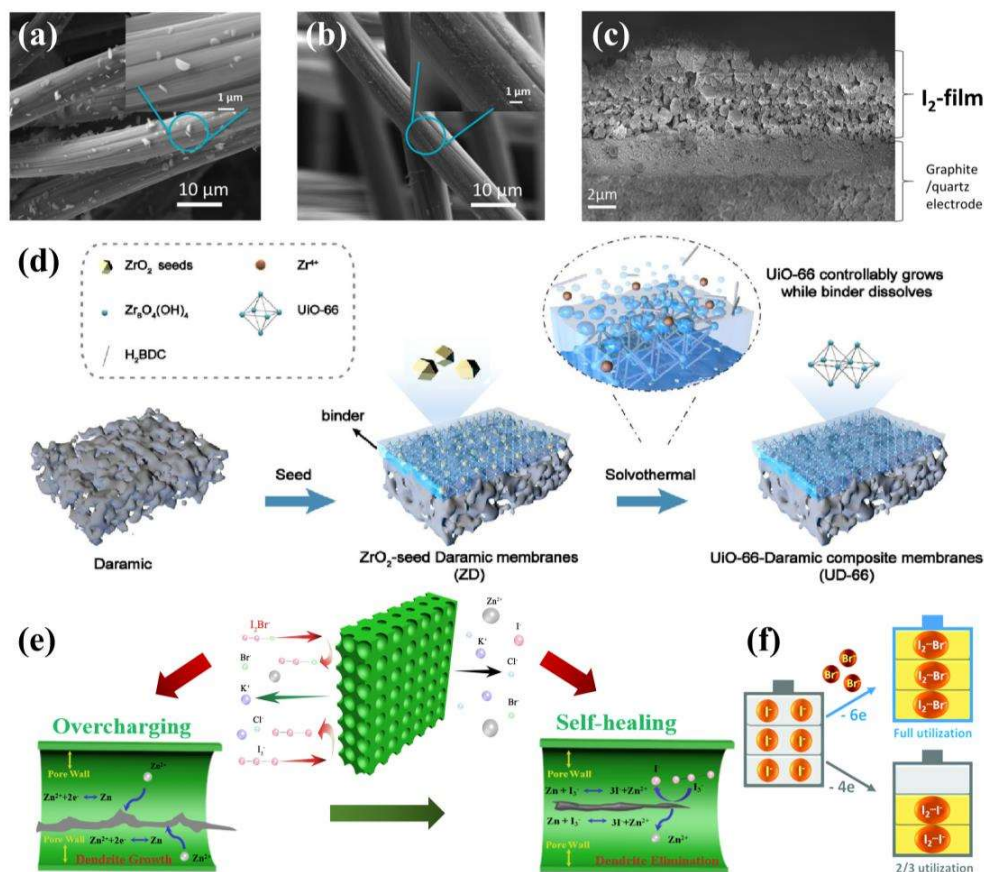


**Fig. 7.** SEM images of (a) MIL-125-NH<sub>2</sub>-modified GFs and (b) UiO-66-CH<sub>3</sub>-modified GFs. Reproduced with permission from Ref. [186]. Copyright 2016, American Chemical Society. (c) Cryo-SEM image for the cross section of the I<sub>2</sub> film formed on the graphite/quartz composite electrode during chronoamperometry for 30 s. Reproduced with permission from Ref. [187]. Copyright 2021, American Chemical Society. (d) Schematic illustration of the BRSM. Reproduced with permission from Ref. [190]. Copyright 2020, Elsevier. (e) Schematic illustration of the overcharging and self-healing process in ZIFB with the porous polyolefin membrane. Reproduced with permission from Ref. [192]. Copyright 2018, Wiley-VCH. (f) Schematic illustration of Br<sup>-</sup> as the complexing agent to stabilize

iodine. Reproduced with permission from Ref. [193]. Copyright 2017, Royal Society of Chemistry.

### 3.3.3 Sn-I<sub>2</sub> flow batteries

Although Zn metal offers a high specific capacity and low cost, it suffers from notorious dendrite formation and side reactions. Therefore, efforts have been dedicated to developing dendrite-free metal electrodes. Sn metal, which exhibits less differences in surface energy between different facets than Zn, is expected to be more isotropic in morphology during electrodeposition. Accordingly, Yao et al. [199] reported an alkaline Sn(OH)<sub>6</sub><sup>2-</sup>/Sn redox couple and paired with I<sub>3</sub><sup>-</sup>/I<sup>-</sup>, forming a Sn-I RFB with reversible cell voltage of 1.4 V. It was shown that the Sn anode in alkaline negolyte achieved dendrite-free and smooth morphology during electrodeposition even at higher current densities and areal capacities due to its intrinsic low surface energy anisotropy and isotropic crystal growth mechanism, leading to superior cycling stability. Consequently, the Sn-I<sub>2</sub> RFB can operate at a high areal capacity of 73.07 mAh cm<sup>-2</sup> for 350 h with no degradation, outperforming the reported ZIFB. In addition, the low Young's modulus ( $E_{\text{Sn}} \approx 42$  GPa) of Sn makes it less likely to penetrate the membrane and cause a short circuit. However, the use of different electrolytes, particularly different pH, in negative and positive sides poses a challenge in the long-term stability of the RFBs. Although adopting a neutral or acidic negative electrolyte for Sn metal may alleviate this issue as demonstrated in the Sn-Br<sub>2</sub> RFB, the cell voltage and energy density may be greatly reduced.

### 3.3.4 Li-I<sub>2</sub> flow batteries

As mentioned in Section 3.2.6, Li metal is one of the most promising anodes and similarly, iodine cathode has been paired with Li metal anode to form Li-I<sub>2</sub> aqueous flow battery. Zhao and Byon demonstrated that a Li-I<sub>2</sub> flow battery can provide over 7 times larger capacity than its static counterpart and decent cyclic performance [200]. To further boost the volumetric capacity, Chen and Lu [201] combined the highly soluble LiI in the liquid phase and high-capacity S/C composite in the solid phase to form a multiple redox semi-solid-liquid (MRSSL) catholyte as shown in **Fig. 8a**, which enabled the RFB to achieve a volumetric capacity of as high as 550 Ah L<sup>-1</sup> and high energy density of 580 Wh L<sup>-1</sup>. It is worth noting that the LiI solution can increase the volumetric capacity of catholyte, improve the electrochemical utilization of S/C composite and reduce the viscosity of catholyte. The MRSSL concept offers a new direction to develop high-energy-density RFB by breaking the solubility of active species and creating synergistic interactions between multiple redox couples. It should be noted that the capacity of these hybrid iodine-based RFBs are limited by the amount of deposited Li metal at the anode. To address this issue, Wang et al. [202] proposed and demonstrated a flexible solid flow electrode (SFE) in the negative side to transport active materials. As illustrated in **Fig. 8b**, a flexible lithium titanium phosphate (LTP) anode belt is rolling to the cell for electrochemical reactions. The energy of the system can be scaled up with the belt length. This unique design allows the use of high-capacity solid electrode while maintaining the design flexibility of energy and power of RFBs. As a proof of concept, the LTP-LiI flow battery exhibited a stable discharge voltage and capacity over 180 cycles. This strategy can be readily



1 applied to other flow battery systems, such as Zn-Br<sub>2</sub>, Zn-I<sub>2</sub> and Li-polysulfide RFBs  
2  
3 which require improvement of the scalability. However, more investigations on the  
4  
5 electrode construction and system design are needed to expand the SFE for practical  
6  
7 applications.  
8  
9

10  
11 To sum up, with the advantages of natural abundance, environmental friendliness  
12  
13 and high solubility of polyiodide ions, iodine has shown great promise as cathode  
14  
15 materials for next-generation high-energy-density RFBs. However, the use of high  
16  
17 concentration electrolyte will lead to a high viscosity and low conductivity, thereby  
18  
19 resulting in large polarizations of iodine-based RFBs. Future studies are needed to  
20  
21 design advanced porous electrodes and cell structure to minimize the ohmic and mass  
22  
23 transport losses. In addition, it is also desired to develop electrode materials with high  
24  
25 surface area and electrocatalytic activity to improve the iodine/iodide reaction kinetics.  
26  
27 Although iodine exists as polyiodide species in aqueous phase and is believed to be  
28  
29 less toxic and corrosive compared to bromine, it may also present a safety concern if  
30  
31 it is employed as a grid scale. Therefore, the stability of polyiodide should be studied  
32  
33 in the future.  
34  
35  
36  
37  
38  
39  
40  
41  
42

#### 43 **4. Halogen as redox mediators**

44  
45 Apart from serving as active materials, halogen species can also act as a redox  
46  
47 mediator to enable novel and high-performance rechargeable batteries. For instance,  
48  
49 LiBr and LiI have been used as a redox mediator to improve the reachability of Li-O<sub>2</sub>  
50  
51 batteries by reducing charging overpotential and inhibiting side reactions [203,204].  
52  
53 Moreover, in Zn-MnO<sub>2</sub> batteries, bromine mediator can not only facilitate the  
54  
55  
56  
57  
58  
59  
60  
61  
62  
63  
64  
65

dissolution of overdeposited  $\text{MnO}_2$  to improve the reversibility of  $\text{MnO}_2/\text{Mn}^{2+}$  reactions, but also increase the battery areal capacity [205]. Similarly, the mixture of  $\text{Mn}^{2+}$  and  $\text{Br}^-$  was proposed for the catholyte of Cd/Br-Mn flow batteries due to the chemical-electrochemical reaction between “dead”  $\text{MnO}_2$  precipitation and  $\text{Br}^-$  in an acidic environment. The assembled flow battery adopting  $\text{Br}^-$  as a redox mediator delivered an EE of  $\sim 76\%$  at  $80 \text{ mA cm}^{-2}$  with the energy density of  $360 \text{ Wh L}^{-1}$ . Moreover, the flow battery paired with silicotungstic acid as anode could continuously run for more than 2000 cycles without obvious capacity decay, which further verified the reliability and versatility of this mixed catholyte [206]. In addition, iodine species have also been reported as redox mediators in lithium-ion batteries, dye-sensitized solar cells, and supercapacitors [207–210]. This section mainly focuses on the application of halogen species as redox mediators in RFBs.

Qing Wang’s group first proposed the redox targeting flow batteries, in which the energy is stored in solid active materials in the external tanks while the electron transfer between electrode and the active material is accomplished by the redox mediator [211]. For example, as illustrated in **Fig. 8c**, a Li- $\text{I}_2$  RFB consists of a Li metal anode and an iodide catholyte with  $\text{LiFePO}_4$  as a solid energy storage material separated by a Nafion membrane [212]. During charging process,  $\text{I}_3^-$  is oxidized at the positive electrode to  $\text{I}_2$ , which is circulated to the reservoir to chemically react with  $\text{LiFePO}_4$ , releasing  $\text{Li}^+$  ions to electrolyte. During discharging, the  $\text{I}_3^-$  is electrochemically reduced to  $\text{I}^-$ , which helps  $\text{Li}^+$  ions to be intercalated into  $\text{FePO}_4$ . This Li- $\text{I}_2$  RFB system with solid  $\text{LiFePO}_4$  exhibits the advantage of high storage

capacity of  $\text{Li}^+$  in the reservoir tank, delivering a high theoretical energy density of 670 Wh  $\text{L}^{-1}$  and capacity retention of 90% after 40 cycles with a high CE of 99% [212]. In addition to traditional Li- $\text{I}_2$  RFBs, based on the redox mediator strategy, Lei et al. [213] introduced  $\text{I}_3^-/\text{I}^-$  to promote the dissolution of  $\text{MnO}_2$  and recover the capacity decay from exfoliated  $\text{MnO}_2$ , thereby improving the cycle stability with high energy efficiency and areal capacity. Specifically,  $\text{I}^-$  ions can chemically react with the residual  $\text{MnO}_2$  deposited on or exfoliated from the CF to form  $\text{Mn}^{2+}$  and  $\text{I}_3^-$ , which can then be electrochemically reduced back to  $\text{I}^-$  on the electrode to complete a mediation cycle. This redox-mediating process facilitates  $\text{MnO}_2$  dissolution effectively, which enables the Zn-Mn RFB to operate at the areal capacity of 15 mAh  $\text{cm}^{-2}$  for 225 cycles.

The  $\text{I}_3^-/\text{I}^-$  redox couples have also been widely used in dye sensitized solar flow cell systems, which are promising next-generation solar energy conversion and storage devices [33,34,214]. Yan et al. [32] proposed a solar rechargeable RFB constructed with dye-sensitized  $\text{TiO}_2$  as photo-anode,  $\text{LiI}$  as cathode in organic electrolyte and  $\text{Li}_2\text{WO}_4$  as anode in aqueous electrolyte separated by a LISICON lithium-ion-conducting glass ceramic film as membrane. After 10 minutes of photo-charging process, the battery can be discharged normally with constant current in the dark environment. On the basis of the proposed working mechanism, Yu et al. [215] demonstrated an integrated Li- $\text{I}_2$  solar flow battery with aqueous catholyte as shown in **Fig. 8d** for the conversion and storage of solar energy. During charging, dye molecules adsorbed on the  $\text{TiO}_2$  surface get photoexcited and inject electrons into the

1 conduction band of  $\text{TiO}_2$  under light illumination. The excited dye molecules are then  
2  
3 reduced along with the oxidation of  $\text{I}^-$  to  $\text{I}_3^-$ , thus achieving solar energy capture and  
4  
5 storage (**Fig. 8e**). The  $\text{I}_3^-$  ions are reduced to  $\text{I}^-$  ions and the captured solar energy is  
6  
7 released in the form of electrical energy during the discharge process. The  
8  
9 dye-sensitized  $\text{TiO}_2$  photoelectrode can provide an external voltage input, and thus the  
10  
11 charging voltage of the battery is reduced from 3.55 to 2.90 V, saving 20% of the  
12  
13 charging energy [216]. In addition, the ethyl viologen diiodide ( $\text{EVI}_2$ ) was used as a  
14  
15 bifunctional redox mediator in a solar rechargeable RFB to simplify the electrolyte  
16  
17 system and bridge a dye-sensitized photoelectrode for integrated solar charging. It is  
18  
19 worth noting that the low-cost Prussian blue (PB) was introduced as an alternative to  
20  
21 the  $\text{LiFePO}_4$   $\text{Li}^+$ -storage material, which enabled the battery to achieve an energy  
22  
23 density of around  $117 \text{ Wh L}^{-1}$  and ensure a stable  $\text{I}_3^-/\text{I}^-$  concentration that is crucial to  
24  
25 the operation of the photoelectrode [217]. Although the power conversion efficiencies  
26  
27 of these solar rechargeable flow batteries are still low, the combination of solar cells  
28  
29 and secondary rechargeable RFBs realizes the conversion and storage of solar energy,  
30  
31 electrical energy and chemical energy in the same system, showing great promise for  
32  
33 large-scale applications [218]. However, there are still several challenging issues to be  
34  
35 solved, such as exploiting alternatives to the low-conductivity brittle ceramic  
36  
37 separator (LISICON) to separate the cathode and anode, improving the conversion  
38  
39 efficiency and operating current density.  
40  
41  
42  
43  
44  
45  
46  
47  
48  
49  
50  
51  
52  
53  
54  
55  
56  
57  
58  
59  
60  
61  
62  
63  
64  
65

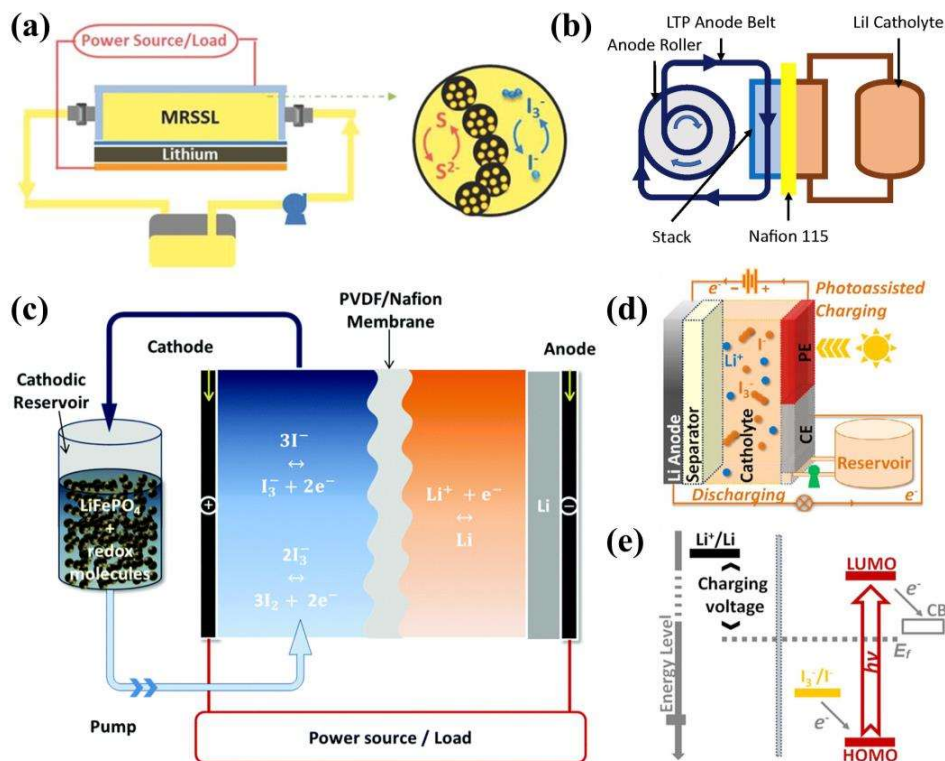


**Fig. 8.** (a) Schematic illustration of a MRSSL flow battery that employs LiI in liquid phase and S/C in solid phase. Reproduced with permission from Ref. [201]. Copyright 2016, Wiley-VCH. (b) Schematic of the LTP-LiI solid-liquid hybrid flow battery using LTP-solid flow electrode. Reproduced with permission from Ref. [202]. Copyright 2019, Elsevier. (c) Schematic of Li-I<sub>2</sub> RFB with solid LiFePO<sub>4</sub>. Reproduced with permission from Ref. [212]. Copyright 2016, Royal Society of Chemistry. (d) Schematic of a Li-I SFB device with the three-electrode configuration; (e) Energy diagram for the photo-assisted charging process. Reproduced with permission from Ref. [215]. Copyright 2015, American Chemical Society.

## 5. Halogen as complexing agents

Another significant role played by halogen species in RFBs is complexing with the active species to increase the energy density and electrochemical performance. In fact,

in halogen-based RFBs, the halogens generated during the charging process are usually complexed with halide ions to form polyhalide ions in aqueous electrolytes, such as  $I_3^-$ ,  $I_2Br^-$ ,  $I_2Cl^-$  and  $Br_2Cl^-$  [194,219,220]. These polyhalide ions have higher solubility than the diatomic molecules, which enable the halogen-based flow batteries to deliver higher energy densities, particular in  $I_2$ -based flow batteries [221]. Moreover, halide ions can also be applied in VRFBs to improve the energy density over the current sulfate electrolyte system. Li et al. [222] proposed a VRFB with sulfate and chloride mixed electrolyte containing 2.5 M  $SO_4^{2-}$  and 6 M  $Cl^-$ , in which four valence states of vanadium ( $V^{2+}$ ,  $V^{3+}$ ,  $V^{4+}$  and  $V^{5+}$ ) were stable up to 2.5 M. They also found that this mixed electrolyte remained stable over a wide temperature range of  $-5 \sim 50$  °C due to the reduction of  $SO_4^{2-}$  concentrations and the formation of soluble neutral complex  $VO_2Cl(H_2O)_2$  above 20 °C, breaking the limitation of the low solubility of  $VOSO_4$  at  $-5$  °C and the precipitation of  $V_2O_5$  at 40 °C. Therefore, a high EE of 87% was achieved during 20 days with a higher energy density of about 40 Wh  $L^{-1}$ . To further understand the mechanism of improved stability of  $V^{5+}$  in mixed acid supporting electrolyte, the Pacific Northwest National Laboratory conducted a series of nuclear magnetic resonance (NMR) spectroscopies and DFT calculations [20,223]. It was found that the formation of  $[V_2O_3Cl_2 \cdot 6H_2O]^{2+}$  complex was more favorable at a higher vanadium concentration ( $\geq 1.75$  M). In particular, the ligand exchange process occurred between the above complex and nearby solvent chlorine molecule to form  $[V_2O_3Cl \cdot 6H_2O]^{2+}$  compound, which was less prone to de-protonation, thus prohibiting the precipitation of  $V_2O_5$  [223]. In addition, they also found that in pure

hydrochloride acid electrolyte,  $V^{5+}$  tends to form vanadium dinuclear ( $[V_2O_3 \cdot 4H_2O]^{4+}$ ) or dinuclear-chloro complexes ( $[V_2O_3Cl \cdot 4H_2O]^{3+}$ ) with good thermal stability in the temperature range of 0 to 50 °C. Moreover, the viscosity of this chloride solution was 30-40% lower than that of the sulfate electrolyte, thus reducing pumping energy loss [224]. Based on previous study, Yang et al. [225] systematically optimized the composition of mixed acid electrolyte (2.4 M vanadium, 6.2 M chloride ion and 2.5 M sulfate), which enabled the VRFB to achieve a high EE and highest energy density at 40-80 mA cm<sup>-2</sup> for more than 100 cycles over a wide temperature range from -20 to 50 °C.

However, the presence of  $Cl^-$  with high concentration increases the risk of chlorine evolution reactions, causing a potential safety hazard for the VRFBs. To address this issue, Zhang et al. [226] proposed to add 0.04 M NaCl as the additive in electrolytes and found that the addition of  $Cl^-$  ions increases the reversibility and lower the charge transfer resistance of  $VO_2^+/VO^{2+}$  redox reactions. The VRFB with an optimal  $Cl^-$  concentration delivers a high EE of 82.5% at 200 mA cm<sup>-2</sup> and a specific discharge capacity of 13.1 Ah L<sup>-1</sup> at 50 mA cm<sup>-2</sup>, reaching up to 98% of the theoretical value. In addition, the improved rate performance and lower capacity decay demonstrate the higher utilization of vanadium ions, which decreases the consumption of vanadium electrolyte and thus reduces the cost of VRFBs.

Furthermore,  $Cl^-$  ions can be served as complexing agents in Cu-based RFBs [227–229]. Sanz et al. [228] investigated the effects of different  $Cl^-$  concentrations and temperatures on the chemical stability of copper chloro-complexes in solution and

the reversibility of electrochemical reactions. They found that the reversibility was improved with temperature. Moreover, in the presence of a high concentration of chloride ions, the potential of  $\text{Cu}^{2+}/\text{Cu}^{+}$  redox couple was increased by 0.5 V compared to the standard redox potential, making it possible to apply as a positive electrolyte for RFBs. Further spectroelectrochemical study and DFT calculations reveal that as the number of chloride ions ( $[\text{CuCl}(\text{H}_2\text{O})_5]^+$ ,  $[\text{CuCl}_2(\text{H}_2\text{O})_4]^0$ , and  $[\text{CuCl}_3(\text{H}_2\text{O})_3]^-$ ) increases, the amount of water molecules available to solvate the metal-ion centers decreases [229]. In addition, the  $\text{Cl}^-$  ions can complex with  $\text{Mn}^{3+}$  ions to inhibit the precipitation of  $\text{MnO}_2$ , which was demonstrated in a low-cost Mn-Fe RFB. By adding HCl into the catholyte, the disproportionation of  $\text{Mn}^{3+}$  has been successfully suppressed due to the formation of  $[\text{MnCl}_4(\text{H}_2\text{O})_2]^-$  complex, which enables the flow battery to deliver a CE of ~100% and run stably at the current density of  $160 \text{ mA cm}^{-2}$  [230].  $\text{Br}^-$  ions can also be used to stabilize zinc ions by  $\text{Zn}^{2+}$ - $\text{Br}^-$  complexation interactions in the near neutral anolytes. By employing KBr as the supporting electrolyte, the reversibility of  $\text{Zn}^{2+}/\text{Zn}$  redox couple was improved due to the complexation interactions and the formation of  $\text{ZnBr}_4^{2-}$  anions confirmed by UV-vis and Raman spectroscopies. Coupled with  $\text{K}_3\text{Fe}(\text{CN})_6$  as the catholyte, the proposed Zn-Fe RFB can achieve a high EE of 86.7% and superior cycling stability over 2000 cycles without obvious capacity degradation at  $30 \text{ mA cm}^{-2}$ , showing great potential for large-scale energy storage [231].

## 6. Summary and Outlook

In summary, the history and recent progress of halogen enabled aqueous flow cells are



summarized and discussed in terms of the role and types of halogen species in this review. It can be seen that bromine- and iodine-based flow cells are attracting more and more attention and considered as promising large-scale energy storage technologies due to their superior characteristics, such as low cost and high energy density, while most chlorine-based flow cells were phased out in the last century. In addition, halogen species can serve as redox mediators and complexing agents, which enable aqueous flow cells to achieve higher energy density and electrochemical performances. Despite the great promise of halogen-based flow cell systems, the following challenges need to be addressed to fully unleash their potential.

First, halogen elements (e.g.,  $\text{Cl}_2$ ,  $\text{Br}_2$ , and  $\text{I}_2$ ) are toxic and corrosive, which presents a significant barrier for the widespread adoption of halogen-based flow batteries. Although the practical application of the  $\text{Br}_2/\text{Br}^-$  couple has been enabled by adding BCAs into the electrolytes, most of these complexing agents are expensive and suffer from reduced complexation ability at elevated temperatures. In addition, the addition of BCAs usually results in the formation of a separate oily polybromide phase at the bottom of the storage tank, which requires complicated system design for pumping the electrolyte and the poor mixing of two phases will lead to low efficiency and fast capacity decay. Therefore, it is of great significance to develop novel BCAs that can firmly sequester bromine while maintaining the electrolyte in a homogeneous phase. For example, 3-chloro-2-hydroxypropyltrimethyl ammonium chloride has demonstrated great promise for this application [173]. Fortunately, iodine is highly soluble in aqueous electrolyte when complexed with halide ions. Nevertheless, further

1 investigations are needed to assess the long-term stability of polyiodide species. It  
2  
3 should be mentioned that safety concern remains a critical barrier to the adoption of  
4  
5 halogen-based RFBs, and future works should be directed to address this issue to  
6  
7 accelerate the commercialization of this technology. Adding halogen complex agents  
8  
9 and developing intelligent battery management systems may be an effective solution  
10  
11 to this challenge.  
12  
13  
14  
15

16  
17 Second, the sluggish kinetics of halogen/halide reactions on common  
18  
19 carbon-based electrodes are one of the main factors hindering the power density and  
20  
21 energy efficiency. Although several strategies have been implemented to improve the  
22  
23 performance of halogen-based RFBs, the mechanisms of halogen/halide reactions  
24  
25 remain unclear. In particular, the electrochemical process may involve various  
26  
27 polyhalide species (e.g.,  $\text{Br}_3^-$ ,  $\text{Br}_5^-$ ) and their complexes with BCAs and/or other  
28  
29 additives. Hence, more fundamental investigations are required to unveil the  
30  
31 underlying physiochemical process, which is essential to the development of  
32  
33 advanced electrodes for high-performance bromine-based RFBs. Integrating in-situ  
34  
35 characterizations (e.g., Raman and nuclear magnetic resonance spectroscopy) and  
36  
37 theoretical calculations (e.g., DFT and molecular dynamics simulations) may be a  
38  
39 powerful approach to this end.  
40  
41  
42  
43  
44  
45  
46  
47  
48  
49

50 Third, it remains a challenge to develop membranes with high ionic conductivity,  
51  
52 high selectivity, high stability and low cost. Currently, perfluorinated cation exchange  
53  
54 membranes, such as Nafion membrane, are widely used due to their high stability and  
55  
56 low active species permeability. However, in addition to the high cost, these  
57  
58  
59  
60  
61  
62  
63  
64  
65

membranes exhibit a low ionic conductivity, particularly when neutral electrolytes are used, leading to a large internal resistance. Low-cost porous separators have been shown to be promising for ZBFBs with the presence of BCAs, but still suffer from severe bromine species crossover. Therefore, it is essential to develop advanced membranes that can meet the stringent requirements. Modifications of existing porous membranes, such as coating or blending with a polymer layer, are a promising research direction. It should be emphasized that understanding the ion transport mechanism through the membrane is also of great significance, which will shed light on the design of micro/nanostructures and materials of membranes.

Finally, to take full advantages of halogen species, it is essential to develop novel negolyte materials with low redox potential and high volumetric capacity. One promising direction for future research is to combine high-throughput DFT and machine learning to rationally screen and design organic molecules with high solubility, fast reaction kinetics, high reversibility and stability.

### **Conflicts of interest**

The authors declare no conflict of interest.

### **Acknowledgment**

The work described in this paper was fully supported by a grant from the Research Grants Council of the Hong Kong Special Administrative Region, China (Project No. 16205721).

### **References**

- [1] Y. Heng, Z. Gu, J. Guo, X. Wu, Research progresses on vanadium-based cathode materials for aqueous zinc-ion batteries, *Acta Phys. -Chim. Sin.* 37

- (2021) 2005013. <https://doi.org/10.3866/PKU.WHXB202005013>.
- [2] T. Nguyen, R.F. Savinell, Flow batteries, *Electrochem. Soc. Interface*. 19 (2010) 54–56. <https://doi.org/10.1149/2.F06103if>.
  - [3] H. Ao, Y. Zhao, J. Zhou, W. Cai, X. Zhang, Y. Zhu, Y. Qian, Rechargeable aqueous hybrid ion batteries: Developments and prospects, *J. Mater. Chem. A*. 7 (2019) 18708–18734. <https://doi.org/10.1039/c9ta06433h>.
  - [4] A. Sepehri, M.H. Sarrafzadeh, Effect of nitrifiers community on fouling mitigation and nitrification efficiency in a membrane bioreactor, *Chem. Eng. Process. Process Intensif.* 128 (2018) 10–18. <https://doi.org/10.1016/j.cep.2018.04.006>.
  - [5] H. Zhang, W. Lu, X. Li, Progress and perspectives of flow battery technologies, *Electrochem. Energy. Rev.* 2 (2019) 492–506. <https://doi.org/10.1007/s41918-019-00047-1>.
  - [6] G.L. Soloveichik, Flow Batteries: Current Status and Trends, *Chem. Rev.* 115 (2015) 11533–11558. <https://doi.org/10.1021/cr500720t>.
  - [7] X. Ding, Q. Huang, X. Xiong, Research and application of fast-charging graphite anodes for lithium-ion batteries, *Acta Phys. -Chim. Sin.* 38 (2022) 2204057. <https://doi.org/10.3866/PKU.WHXB202204057>.
  - [8] Z. Yang, J. Zhang, M.C.W. Kintner-Meyer, X. Lu, D. Choi, J.P. Lemmon, J. Liu, Electrochemical energy storage for green grid, *Chem. Rev.* 111 (2011) 3577–3613. <https://doi.org/10.1021/cr100290v>.
  - [9] G. Cong, Y.C. Lu, Strategies to improve the energy density of non-aqueous organic redox flow batteries, *Acta Phys. -Chim. Sin.* 38 (2022) 2106008. <https://doi.org/10.3866/PKU.WHXB202106008>.
  - [10] W. Wang, Q. Luo, B. Li, X. Wei, L. Li, Z. Yang, Recent progress in redox flow battery research and development, *Adv. Funct. Mater.* 23 (2013) 970–986. <https://doi.org/10.1002/adfm.201200694>.
  - [11] J. Noack, N. Roznyatovskaya, T. Herr, P. Fischer, The chemistry of redox-flow batteries, *Angew. Chem.* 54 (2015) 9776–9809. <https://doi.org/10.1002/anie.201410823>.
  - [12] Z. Li, Y.C. Lu, Material design of aqueous redox flow batteries: fundamental challenges and mitigation strategies, *Adv. Mater.* 32 (2020) 1–30. <https://doi.org/10.1002/adma.202002132>.
  - [13] Z. Xu, M. Jing, J. Liu, C. Yan, X. Fan, Advanced dual-gradient carbon nanofibers/graphite felt composite electrode for the next-generation vanadium flow battery, *J. Mater. Sci. Technol.* 136 (2023) 32–42. <https://doi.org/10.1016/j.jmst.2022.06.051>.
  - [14] G. Kear, A.A. Shahand, F.C. Walsh, Development of the all- vanadium redox flow battery for energy storage: A review of technological, financial and policy aspects, *Int. J. Energy Res.* 36 (2012) 1105–1120. <https://doi.org/10.1002/er.1863>.
  - [15] M. Ulaganathan, V. Aravindan, Q. Yan, S. Madhavi, M. Skyllas-Kazacos, T.M. Lim, Recent advancements in all-vanadium redox flow batteries, *Adv. Mater. Interfaces.* 3 (2016) 1–22. <https://doi.org/10.1002/admi.201500309>.

- [16] Z. Xu, W. Xiao, K. Zhang, D. Zhang, H. Wei, X. Zhang, Z. Zhang, N. Pu, J. Liu, C. Yan, An advanced integrated electrode with micron- and nano-scale structures for vanadium redox flow battery, *J. Power Sources*. 450 (2020) 227686. <https://doi.org/10.1016/j.jpowsour.2019.227686>.
- [17] J. Du, J. Liu, S. Liu, L. Wang, K.C. Chou, Research progress of vanadium battery with mixed acid system: A review, *J. Energy Storage*. 70 (2023) 107961. <https://doi.org/10.1016/j.est.2023.107961>.
- [18] H. Chen, X. Zhang, S. Zhang, S. Wu, F. Chen, J. Xu, A comparative study of iron-vanadium and all-vanadium flow battery for large scale energy storage, *Chem. Eng. J.* 429 (2022) 132403. <https://doi.org/10.1016/j.cej.2021.132403>.
- [19] Z. Xu, M. Zhu, K. Zhang, X. Zhang, L. Xu, J. Liu, T. Liu, C. Yan, Inspired by “quenching-cracking” strategy: Structure-based design of sulfur-doped graphite felts for ultrahigh-rate vanadium redox flow batteries, *Energy Storage Mater.* 39 (2021) 166–175. <https://doi.org/10.1016/j.ensm.2021.04.025>.
- [20] M. Skyllas-Kazacos, L. Cao, M. Kazacos, N. Kausar, A. Mousa, Vanadium electrolyte studies for the vanadium redox battery – A review, *ChemSusChem*. 9 (2016) 1521–1543. <https://doi.org/10.1002/cssc.201600102>.
- [21] S. Berling, J.M. Hidalgo, N. Patil, E. García-Quismondo, J. Palma, C. Ponce de León, A mediated vanadium flow battery: Lignin as redox-targeting active material in the vanadium catholyte, *J. Energy Storage*. 68 (2023). <https://doi.org/10.1016/j.est.2023.107620>.
- [22] K.E. Rodby, R.L. Jaffe, E.A. Olivetti, F.R. Brushett, Materials availability and supply chain considerations for vanadium in grid-scale redox flow batteries, *J. Power Sources*. 560 (2023) 232605. <https://doi.org/10.1016/j.jpowsour.2022.232605>.
- [23] Z. Huang, A. Mu, L. Wu, B. Yang, Y. Qian, J. Wang, Comprehensive analysis of critical issues in all-vanadium redox flow battery, *ACS Sustain. Chem. Eng.* 10 (2022) 7786–7810. <https://doi.org/10.1021/acssuschemeng.2c01372>.
- [24] C. Minke, T. Turek, Materials, system designs and modelling approaches in techno-economic assessment of all-vanadium redox flow batteries - A review, *J. Power Sources*. 376 (2018) 66–81. <https://doi.org/10.1016/j.jpowsour.2017.11.058>.
- [25] P. Zhao, H. Zhang, H. Zhou, J. Chen, S. Gao, B. Yi, Characteristics and performance of 10 kW class all-vanadium redox-flow battery stack, *J. Power Sources*. 162 (2006) 1416–1420. <https://doi.org/10.1016/j.jpowsour.2006.08.016>.
- [26] M. Zhang, M. Moore, J.S. Watson, T.A. Zawodzinski, R.M. Counce, Capital cost sensitivity analysis of an all-vanadium redox-flow battery, *J. Electrochem. Soc.* 159 (2012) A1183–A1188. <https://doi.org/10.1149/2.041208jes>.
- [27] A. Khor, P. Leung, M.R. Mohamed, C. Flox, Q. Xu, L. An, R.G.A. Wills, J.R. Morante, A.A. Shah, Review of zinc-based hybrid flow batteries: From fundamentals to applications, *Mater. Today Energy*. 8 (2018) 80–108. <https://doi.org/10.1016/j.mtener.2017.12.012>.
- [28] Y. Shi, C. Eze, B. Xiong, W. He, H. Zhang, T.M. Lim, A. Ukil, J. Zhao, Recent

- development of membrane for vanadium redox flow battery applications: A review, *Appl. Energy*. 238 (2019) 202–224. <https://doi.org/10.1016/j.apenergy.2018.12.087>.
- [29] Y.V. Tolmachev, Hydrogen-halogen electrochemical cells: A review of applications and technologies, *Russ. J. Electrochem.* 50 (2014) 301–316. <https://doi.org/10.1134/S1023193513120069>.
- [30] S. Zhang, W. Guo, F. Yang, P. Zheng, R. Qiao, Z. Li, Recent progress in polysulfide redox-flow batteries, *Batter. Supercaps.* 2 (2019) 627–637. <https://doi.org/10.1002/batt.201900056>.
- [31] P.C. Butler, P.A. Eidler, P.G. Grimes, S.E. Klassen, R.C. Miles, Zinc/bromine batteries, *Handbook of Batteries* (third ed.), New York (2001), pp. 37.1–37.8.
- [32] N.F. Yan, G.R. Li, X.P. Gao, Solar rechargeable redox flow battery based on  $\text{Li}_2\text{WO}_4/\text{LiI}$  couples in dual-phase electrolytes, *J. Mater. Chem. A*. 1 (2013) 7012–7015. <https://doi.org/10.1039/c3ta11360d>.
- [33] G. Boschloo, A. Hagfeldt, Characteristics of the iodide/triiodide redox mediator in dye-sensitized solar cells, *Acc. Chem. Res.* 42 (2009) 1819–1826. <https://doi.org/10.1021/ar900138m>.
- [34] G. Nikiforidis, K. Tajima, H.R. Byon, High energy efficiency and stability for photoassisted aqueous lithium-iodine redox batteries, *ACS Energy Lett.* 1 (2016) 806–813. <https://doi.org/10.1021/acsenergylett.6b00359>.
- [35] A. Jameson, E. Gyenge, Halogens as positive electrode active species for flow batteries and regenerative fuel cells, *Electrochem. Energy Rev.* 3 (2020) 431–465. <https://doi.org/10.1007/s41918-020-00067-2>.
- [36] J. Jorné, J.T. Kim, D. Kralik, The zinc-chlorine battery: half-cell overpotential measurements, *J. Appl. Electrochem.* 9 (1979) 573–579. <https://doi.org/10.1007/BF00610944>.
- [37] J.T. Kim, J. Jorné, The kinetics of a chlorine graphite electrode in the zinc-chlorine battery, *J. Electrochem. Soc.* 124 (1977) 1473–1477. <https://doi.org/10.1149/1.2133094>.
- [38] R.V. Sbenoy, J.M. Fenton, P. Malachuk and P. Stonehart, Characterization of a porous electrode in a zinc chlorine battery, 136 (1989) 3181–3189. <https://doi.org/10.1149/1.2096423>.
- [39] P.C. Symons, Process for electrical energy using solid halogen hydrates, US Patent 3713888 (1973).
- [40] S. Mitra, A design for zinc-chlorine batteries, *J. Power Sources*. 8 (1982) 359–367. [https://doi.org/10.1016/0378-7753\(82\)80037-2](https://doi.org/10.1016/0378-7753(82)80037-2).
- [41] C.J. Amato, A zinc-chloride battery—The missing link to a practical electric car, *SAE Tech. Pap.* (1973) 730248. <https://doi.org/10.4271/730248>.
- [42] M. Futamata, S. Higuchi, I. Ogino, Y. Takada, S. Okazaki, S. Ashimura, S. Takahashi, Performance testing of 10 kW-class advanced batteries for electric energy storage system in Japan, *J. Power Sources*. 24 (1988) 137–155. [https://doi.org/10.1016/0378-7753\(88\)80098-3](https://doi.org/10.1016/0378-7753(88)80098-3).
- [43] Y. Misawa, A. Suzuki, S. Shimizu, H. Sato, K. Ashizawa, T. Sumii, M. Ohtomo, Demonstration test of a 60 kW-class zinc/chlorine battery as a power

- storage system, Proceedings of the 24th IECEC, Washington D.C., IEEE, (1989) 1325–1329. <https://doi.org/10.1109/IECEC.1989.74640>.
- [44] R.G. Zalosh, S.N. Bajpai, T.P. Short, R.K. Tsui, Chlorine hazard evaluation for the zinc-chlorine electric vehicle battery, Final technical report. [50 kWh]. United States, 1980. <https://doi.org/10.2172/5273405>.
- [45] E. Lorbeer, A hazard assessment of zinc-chlorine electric vehicle batteries, J. Power Sources. 5(4) (1979) 398–399. [https://doi.org/10.1016/0378-7753\(80\)80071-1](https://doi.org/10.1016/0378-7753(80)80071-1).
- [46] S. Yoshizawa, Z. Takehara, Y. Ito, Y. Nakanishi, Y. Koyama, Recovery of electric power by direct chlorination of hydrogen or hydrocarbons in a high temperature fuel cell, J. Appl. Electrochem. 4 (1974) 81–85. <https://doi.org/10.1007/BF00615909>.
- [47] D.L. Maricle, Hydrogen/chlorine regenerative fuel cell, US Patent 4128701 (1978).
- [48] G.L. Soloveichik, Regenerative fuel cells for energy storage, Proc. IEEE. 102 (2014) 964–975. <https://doi.org/10.1109/JPROC.2014.2314955>.
- [49] K.T. Cho, M.C. Tucker, A.Z. Weber, A review of hydrogen/halogen flow cells, Energy Technol. 4 (2016) 655–678. <https://doi.org/10.1002/ente.201500449>.
- [50] S.K. Mondal, J. Rugolo, M.J. Aziz, Alloy oxide electrocatalysts for regenerative hydrogen-halogen fuel cell, Mater. Res. Soc. Symp. Proc. 1311 (2011) 19–24. <https://doi.org/10.1557/opl.2011.108>.
- [51] D.T. Chin, R.S. Yeo, J. McBreen, S. Srinivasan, An electrochemically regenerative hydrogen- chlorine energy storage system: A study of mass and heat balances, J. Electrochem. Soc. 126 (1979) 713–720. <https://doi.org/10.1149/1.2129126>.
- [52] R.S. Yeo, J. McBreen, Transport properties of Nafion membranes in electrochemically regenerative hydrogen/halogen cells, J. Electrochem. Soc. 126 (1979) 1682–1687. <https://doi.org/10.1149/1.2128776>.
- [53] R.S. Yeo, J. McBreen, A.C.C. Tseung, S. Srinivasan, J. McElroy, An electrochemically regenerative hydrogen-chlorine energy storage system: electrode kinetics and cell performance, J. Appl. Electrochem. 10 (1980) 393–404. <https://doi.org/10.1007/BF00617215>.
- [54] M. Carvela, A. Raschitor, M.A. Rodrigo, J. Lobato, Recent progress in catalysts for hydrogen-chlorine regenerative fuel cells, Catalysts. 10 (2020) 1–22. <https://doi.org/10.3390/catal10111263>.
- [55] M. Thomassen, B. Børresen, G. Hagen, R. Tunold, H<sub>2</sub>/Cl<sub>2</sub> fuel cell for co-generation of electricity and HCl, J. Appl. Electrochem. 33 (2003) 9–13. <https://doi.org/10.1023/A:1022942213808>.
- [56] S.M.A. Shibli, M. Noel, Platinum-iridium bimetal catalyst-based porous carbon electrodes for H<sub>2</sub>-Cl<sub>2</sub> fuel cells, Int. J. Hydrogen Energy. 18 (1993) 141–147. [https://doi.org/10.1016/0360-3199\(93\)90200-T](https://doi.org/10.1016/0360-3199(93)90200-T).
- [57] J. Rugolo, B. Huskinson, M.J. Aziz, Model of performance of a regenerative hydrogen chlorine fuel cell for grid-scale electrical energy storage, J. Electrochem. Soc. 159 (2011) 133–144. <https://doi.org/10.1149/2.030202jes>.

- [58] B. Huskinson, J. Rugolo, S.K. Mondal, M.J. Aziz, A high power density, high efficiency hydrogen-chlorine regenerative fuel cell with a low precious metal content catalyst, *Energy Environ. Sci.* 5 (2012) 8690–8698. <https://doi.org/10.1039/c2ee22274d>.
- [59] M. Carvela, J. Lobato, M.A. Rodrigo, Storage of energy using a gas-liquid H<sub>2</sub>/Cl<sub>2</sub> fuel cell: A first approach to electrochemically-assisted absorbers, *Chemosphere*. 254 (2020) 126795. <https://doi.org/10.1016/j.chemosphere.2020.126795>.
- [60] S. Liu, H. Yu, L. Zhou, P. Wang, Z. Shao, B. Yi, Silicon modified ultrafiltration-based proton-conductive membranes with improved performance for H<sub>2</sub>/Cl<sub>2</sub> fuel cell application, *Int. J. Hydrogen Energy*. 37 (2012) 11425–11430. <https://doi.org/10.1016/j.ijhydene.2012.04.096>.
- [61] S. Liu, L. Zhou, P. Wang, L. Zhang, Z. Shao, B. Yi, Poly(ether sulfone)-sulfonated poly(ether ether ketone) blend ultrafiltration/nanofiltration-based proton-conductive membranes with improved performance for H<sub>2</sub>/Cl<sub>2</sub> fuel cell application, *J. Mater. Chem.* 22 (2012) 20512–20519. <https://doi.org/10.1039/c2jm33804a>.
- [62] S. Liu, L. Zhou, P. Wang, Z. Shao, B. Yi, Nonhumidified high temperature H<sub>2</sub>/Cl<sub>2</sub> fuel cells using protic ionic liquids, *J. Mater. Chem. A*. 1 (2013) 4423–4426. <https://doi.org/10.1039/c2ta00924b>.
- [63] S. Hou, L. Chen, X. Fan, X. Fan, X. Ji, B. Wang, C. Cui, J. Chen, C. Yang, W. Wang, C. Li, C. Wang, High-energy and low-cost membrane-free chlorine flow battery, *Nat. Commun.* 13 (2022) 1–8. <https://doi.org/10.1038/s41467-022-28880-x>.
- [64] C.S. Bradley, Secondary battery, US Patent 312802A (1885).
- [65] A.M.L. and R.C.K. H.S.Lim, Zinc- bromine secondary battery, *J. Electrochem. Soc.* 124 (1977) 1154.
- [66] X. Li, C. Ponce-de-Léon, F.C. Walsh, R.G.A. Wills, D. Pletcher, Zinc-based flow batteries for medium- and large-scale energy storage, *Advances in batteries for medium and large-scale energy storage*. (2015) 293–315. <https://doi.org/10.1016/B978-1-78242-013-2.00008-X>.
- [67] N.H. Clark, P. Eidler, Development of zinc/bromine batteries for load-leveling applications: Phase 2 final report, United States, (1999). <https://doi.org/10.2172/14816>.
- [68] P. Eidler, Development of zinc/bromine batteries for load-leveling applications: Phase 1 final report, United States, (1999). <https://doi.org/10.2172/9466>.
- [69] C. Ponce-de-León, A. Frías-Ferrer, J. González-García, D.A. Szánto, F.C. Walsh, Redox flow cells for energy conversion, *J. Power Sources*. 160 (2006) 716–732. <https://doi.org/10.1016/j.jpowsour.2006.02.095>.
- [70] T. Fujii, M. Igarashi, K. Fushimi, T. Hashimoto, A. Hirota, H. Itoh, K. Jin-Nai, Y. Tagami, I. Kouzuma, Y. Sera, T. Nakayam, 4 MW zinc-bromine battery for electric power storage, *Energy Conversion Engineering Conference*. 3 (1989) 1319–1323. <https://doi.org/10.1109/IECEC.1989.74639>.
- [71] A. Li, J. Li, Y. He, M. Wu, Toward stable and highly reversible zinc anodes for



- aqueous batteries via electrolyte engineering, *J. Energy Chem.* (2023). <https://doi.org/10.1016/j.jechem.2023.04.006>.
- [72] Z. Xu, Q. Fan, Y. Li, J. Wang, P.D. Lund, Review of zinc dendrite formation in zinc bromine redox flow battery, *Renew. Sustain. Energy Rev.* 127 (2020) 109838. <https://doi.org/10.1016/j.rser.2020.109838>.
- [73] L. Guo, H. Guo, H. Huang, S. Tao, Y. Cheng, Inhibition of zinc dendrites in zinc-based flow batteries, *Front. Chem.* 8 (2020) 1–8. <https://doi.org/10.3389/fchem.2020.00557>.
- [74] H. Zhang, W. Lu, X. Li, Progress and perspectives of flow battery technologies, *Electrochem. Energy Rev.* 2 (2019) 492–506. <https://doi.org/10.1007/s41918-019-00047-1>.
- [75] Z. Yuan, Y. Yin, C. Xie, H. Zhang, Y. Yao, X. Li, Advanced materials for zinc-based flow battery: development and challenge, *Adv. Mater.* 31 (2019) 1–27. <https://doi.org/10.1002/adma.201902025>.
- [76] G. Wang, H. Zou, X. Zhu, M. Ding, C. Jia, Recent progress in zinc-based redox flow batteries: A review, *J. Phys. D. Appl. Phys.* 55 (2022). <https://doi.org/10.1088/1361-6463/ac4182>.
- [77] Z. Xu, M. Wu, Toward dendrite-free deposition in zinc-based flow batteries: status and prospects, *Batteries.* 8 (2022) 1–23. <https://doi.org/10.3390/batteries8090117>.
- [78] E. Lancry, B-Z. Magnes, I. Ben-David, M. Freiberg, New bromine complexing agents for bromide based batteries, *ECS Trans.* 53 (2013) 107–115. <https://doi.org/10.1149/05307.0107ecst>.
- [79] K.J. Cathro, K. Cedzynska, D.C. Constable, P.M. Hoobin, Selection of quaternary ammonium bromides for use in zinc/bromine cells, *J. Power Sources.* 18 (1986) 349–370. [https://doi.org/10.1016/0378-7753\(86\)80091-X](https://doi.org/10.1016/0378-7753(86)80091-X).
- [80] D.J. Eustace, Bromine complexation in zinc-bromine circulating batteries, *J. Electrochem. Soc.* 127 (1980) 528–532. <https://doi.org/10.1149/1.2129706>.
- [81] S.C. Leach, C.M. Ablow, K. Kinoshita, Mathematical analysis of axisymmetric sessile drop: Application to the reduction of bromine in a two-phase electrolyte, *J. Colloid Interface Sci.* 92 (1983) 489–498. [https://doi.org/10.1016/0021-9797\(83\)90170-4](https://doi.org/10.1016/0021-9797(83)90170-4).
- [82] M. Schneider, G.P. Rajarathnam, M.E. Easton, A.F. Masters, T. Maschmeyer, A.M. Vassallo, The influence of novel bromine sequestration agents on zinc/bromine flow battery performance, *RSC Adv.* 6 (2016) 110548–110556. <https://doi.org/10.1039/c6ra23446a>.
- [83] D. Bryans, B.G. McMillan, M. Spicer, A. Wark, L. Berlouis, Complexing additives to reduce the immiscible phase formed in the hybrid ZnBr<sub>2</sub> flow battery, *J. Electrochem. Soc.* 164 (2017) A3342–A3348. <https://doi.org/10.1149/2.1651713jes>.
- [84] J.H. Yang, H.S. Yang, H.W. Ra, J. Shim, J.D. Jeon, Effect of a surface active agent on performance of zinc/bromine redox flow batteries: Improvement in current efficiency and system stability, *J. Power Sources.* 275 (2015) 294–297. <https://doi.org/10.1016/j.jpowsour.2014.10.208>.

- [85] D. Kim, J. Jeon, Study on durability and stability of an aqueous electrolyte solution for zinc bromide hybrid flow batteries, *J. Phys. Conf. Ser.* 574 (2014) 012074. <https://doi.org/10.1088/1742-6596/574/1/012074>.
- [86] M.C. Wu, T.S. Zhao, H.R. Jiang, Y.K. Zeng, Y.X. Ren, High-performance zinc bromine flow battery via improved design of electrolyte and electrode, *J. Power Sources.* 355 (2017) 62–68. <https://doi.org/10.1016/j.jpowsour.2017.04.058>.
- [87] R.V. Adith, R. pandiyan Naresh, K. Mariyappan, M. Ulaganathan, P. Ragupathy, An optimistic approach on flow rate and supporting electrolyte for enhancing the performance characteristics of Zn-Br<sub>2</sub> redox flow battery, *Electrochim. Acta.* 388 (2021) 138451. <https://doi.org/10.1016/j.electacta.2021.138451>.
- [88] M.C. Wu, T.S. Zhao, L. Wei, H.R. Jiang, R.H. Zhang, Improved electrolyte for zinc-bromine flow batteries, *J. Power Sources.* 384 (2018) 232–239. <https://doi.org/10.1016/j.jpowsour.2018.03.006>.
- [89] M. Li, H. Su, Q. Qiu, G. Zhao, Y. Sun, W. Song, A quaternized polysulfone membrane for zinc-bromine redox flow battery, *J. Chem.* 2014 (2014) 321629. <https://doi.org/10.1155/2014/321629>.
- [90] R.P. Naresh, P. Ragupathy, M. Ulaganathan, Carbon nanotube scaffolds entrapped in a gel matrix for realizing the improved cycle life of zinc bromine redox flow batteries, *ACS Appl. Mater. Interfaces.* 13 (2021) 48110–48118. <https://doi.org/10.1021/acsami.1c14324>.
- [91] R. Kim, H.G. Kim, G. Doo, C. Choi, S. Kim, J.H. Lee, J. Heo, H.Y. Jung, H.T. Kim, Ultrathin Nafion-filled porous membrane for zinc/bromine redox flow batteries, *Sci. Rep.* 7 (2017) 1–8. <https://doi.org/10.1038/s41598-017-10850-9>.
- [92] L. Hua, W. Lu, T. Li, P. Xu, H. Zhang, X. Li, A highly selective porous composite membrane with bromine capturing ability for a bromine-based flow battery, *Mater. Today Energy.* 21 (2021) 100763. <https://doi.org/10.1016/j.mtener.2021.100763>.
- [93] D. Han, S. Shanmugam, Active material crossover suppression with bi-ionic transportability by an amphoteric membrane for zinc–bromine redox flow battery, *J. Power Sources.* 540 (2022) 231637. <https://doi.org/10.1016/j.jpowsour.2022.231637>.
- [94] Y. Popat, D. Trudgeon, C. Zhang, F.C. Walsh, P. Connor, X. Li, Carbon materials as positive electrodes in bromine-based flow batteries, *Chempluschem.* 87 (2022) . <https://doi.org/10.1002/cplu.202100441>.
- [95] T. Jiang, H. Lin, Q. Sun, G. Zhao, J. Shi, Recent progress of electrode materials for zinc bromide flow battery, *Int. J. Electrochem. Sci.* 13 (2018) 5603–5611. <https://doi.org/10.20964/2018.06.34>.
- [96] K.J. Cathro, K. Cedzynska, D.C. Constable, Preparation and performance of plastic-bonded-carbon bromine electrodes, *J. Power Sources.* 19 (1987) 337–356. [https://doi.org/10.1016/0378-7753\(87\)87009-X](https://doi.org/10.1016/0378-7753(87)87009-X).
- [97] M. Futamata, T. Takeuchi, Deterioration mechanism of the carbon-plastic electrode of the Zn-Br<sub>2</sub> battery, *Carbon.* 30 (1992) 1047–1053. <https://doi.org/>

- 10.1016/0008-6223(92)90135-J.
- [98] L. Zhang, H. Zhang, Q. Lai, X. Li, Y. Cheng, Development of carbon coated membrane for zinc/bromine flow battery with high power density, *J. Power Sources*. 227 (2013) 41–47. <https://doi.org/10.1016/j.jpowsour.2012.11.033>.
- [99] C. Wang, X. Li, X. Xi, P. Xu, Q. Lai, H. Zhang, Relationship between activity and structure of carbon materials for  $\text{Br}_2/\text{Br}^-$  in zinc bromine flow batteries, *RSC Adv.* 6 (2016) 40169–40174. <https://doi.org/10.1039/C6RA03712G>
- [100] C. Wang, Q. Lai, P. Xu, D. Zheng, X. Li, H. Zhang, Cage-like porous carbon with superhigh activity and  $\text{Br}_2$ -complex-entrapping capability for bromine-based flow batteries, *Adv. Mater.* 29 (2017) 1–6. <https://doi.org/10.1002/adma.201605815>.
- [101] C. Wang, X. Li, X. Xi, W. Zhou, Q. Lai, H. Zhang, Bimodal highly ordered mesostructure carbon with high activity for  $\text{Br}_2/\text{Br}^-$  redox couple in bromine based batteries, *Nano Energy*. 21 (2016) 217–227. <https://doi.org/10.1016/j.nanoen.2016.01.015>.
- [102] C. Wang, Q. Lai, K. Feng, P. Xu, X. Li, H. Zhang, From zeolite-type metal organic framework to porous nano-sheet carbon: High activity positive electrode material for bromine-based flow batteries, *Nano Energy*. 44 (2018) 240–247. <https://doi.org/10.1016/j.nanoen.2017.12.007>.
- [103] K. Mariyappan, R. Velmurugan, B. Subramanian, P. Ragupathy, M. Ulaganathan, Low loading of Pt@graphite felt for enhancing multifunctional activity towards achieving high energy efficiency of Zn– $\text{Br}_2$  redox flow battery, *J. Power Sources*. 482 (2021) 228912. <https://doi.org/10.1016/j.jpowsour.2020.228912>.
- [104] Y. Munaiah, S. Dheenadayalan, P. Ragupathy, V.K. Pillai, High performance carbon nanotube based electrodes for zinc bromine redox flow batteries, *ECS J. Solid State Sci. Technol.* 2 (2013) M3182–M3186. <https://doi.org/10.1149/2.024310jss>.
- [105] Y. Munaiah, S. Suresh, S. Dheenadayalan, V.K. Pillai, P. Ragupathy, Comparative electrocatalytic performance of single-walled and multiwalled carbon nanotubes for zinc bromine redox flow batteries, *J. Phys. Chem. C*. 118 (2014) 14795–14804. <https://doi.org/10.1021/jp503287r>.
- [106] S. Suresh, M. Ulaganathan, R. Pitchai, Realizing highly efficient energy retention of Zn– $\text{Br}_2$  redox flow battery using rGO supported 3D carbon network as a superior electrode, *J. Power Sources*. 438 (2019) 226998. <https://doi.org/10.1016/j.jpowsour.2019.226998>.
- [107] M.C. Wu, H.R. Jiang, R.H. Zhang, L. Wei, K.Y. Chan, T.S. Zhao, N-doped graphene nanoplatelets as a highly active catalyst for  $\text{Br}_2/\text{Br}^-$  redox reactions in zinc-bromine flow batteries, *Electrochim. Acta*. 318 (2019) 69–75. <https://doi.org/10.1016/j.electacta.2019.06.064>.
- [108] M.C. Wu, R.H. Zhang, K. Liu, J. Sun, K.Y. Chan, T.S. Zhao, Mesoporous carbon derived from pomelo peel as a high-performance electrode material for zinc-bromine flow batteries, *J. Power Sources*. 442 (2019). <https://doi.org/10.1016/j.jpowsour.2019.227255>.

- [109] L. Tang, T. Li, W. Lu, X. Li, Lamella-like electrode with high Br<sub>2</sub>-entrapping capability and activity enabled by adsorption and spatial confinement effects for bromine-based flow battery, *Sci. Bull.* 67 (2022) 1362–1371. <https://doi.org/10.1016/j.scib.2022.05.012>.
- [110] S. Suresh, M. Ulaganathan, R. Aswathy, P. Ragupathy, Enhancement of bromine reversibility using chemically modified electrodes and their applications in zinc bromine hybrid redox flow batteries, *ChemElectroChem*. 5 (2018) 3411–3418. <https://doi.org/10.1002/celec.201801149>.
- [111] K.S. Archana, R. pandiyan Naresh, H. Enale, V. Rajendran, A.M.V. Mohan, A. Bhaskar, P. Ragupathy, D. Dixon, Effect of positive electrode modification on the performance of zinc-bromine redox flow batteries, *J. Energy Storage*. 29 (2020) 101462. <https://doi.org/10.1016/j.est.2020.101462>.
- [112] R. pandiyan Naresh, A. Surendran, P. Ragupathy, D. Dixon, Enhanced electrochemical performance of zinc/bromine redox flow battery with carbon-nanostructured felt generated by cobalt ions, *J. Energy Storage*. 52 (2022) 104913. <https://doi.org/10.1016/j.est.2022.104913>.
- [113] W. Lu, P. Xu, S. Shao, T. Li, H. Zhang, X. Li, Multifunctional carbon felt electrode with N-Rich defects enables a long-cycle zinc-bromine flow battery with ultrahigh power density, *Adv. Funct. Mater.* 31 (2021) 1–10. <https://doi.org/10.1002/adfm.202102913>.
- [114] C. Wang, W. Lu, Q. Lai, P. Xu, H. Zhang, X. Li, A TiN nanorod array 3D hierarchical composite electrode for ultrahigh-power-density bromine-based flow batteries, *Adv. Mater.* 31 (2019) 1–8. <https://doi.org/10.1002/adma.201904690>.
- [115] W. Glass, G.H. Boyle, Performance of hydrogen-bromine fuel cells, *Fuel Cell Systems*. 47 (1969) 203–220. <https://doi.org/10.1021/ba-1965-0047.ch015>.
- [116] K. Oh, A.Z. Weber, H. Ju, Study of bromine species crossover in H<sub>2</sub>/Br<sub>2</sub> redox flow batteries, *Int. J. Hydrogen Energy*. 42 (2017) 3753–3766. <https://doi.org/10.1016/j.ijhydene.2016.12.063>.
- [117] K. Saadi, S.S. Hardisty, Z. Tatus-Portnoy, D. Zitoun, Influence of loading, metallic surface state and surface protection in precious group metal hydrogen electrocatalyst for H<sub>2</sub>/Br<sub>2</sub> redox-flow batteries, *J. Power Sources*. 536 (2022) 231494. <https://doi.org/10.1016/j.jpowsour.2022.231494>.
- [118] K. Saadi, P. Nanikashvili, Z. Tatus-Portnoy, S. Hardisty, V. Shokhen, M. Zysler, D. Zitoun, Crossover-tolerant coated platinum catalysts in hydrogen/bromine redox flow battery, *J. Power Sources*. 422 (2019) 84–91. <https://doi.org/10.1016/j.jpowsour.2019.03.043>.
- [119] L. Tang, W. Lu, H. Zhang, X. Li, Progress and perspective of the cathode materials towards bromine-based flow batteries, *Energy Mater. Adv.* 2022 (2022). <https://doi.org/10.34133/2022/9850712>.
- [120] K.T. Cho, P. Ridgway, A.Z. Weber, S. Haussener, V. Battaglia, V. Srinivasan, High performance hydrogen/bromine redox flow battery for grid-scale energy storage, *J. Electrochem. Soc.* 159 (2012) A1806–A1815. <https://doi.org/10.1149/2.018211jes>.

- [121] V. Yarlagadda, G. Lin, P.Y. Chong, T. Van Nguyen, High surface area carbon electrodes for bromine reactions in H<sub>2</sub>/Br<sub>2</sub> fuel cells, *J. Electrochem. Soc.* 163 (2016) A5126–A5133. <https://doi.org/10.1149/2.0171601jes>.
- [122] V. Yarlagadda, G. Lin, P.Y. Chong, T. Van Nguyen, High active surface area and durable multi-wall carbon nanotube-based electrodes for the bromine reactions in H<sub>2</sub>-Br<sub>2</sub> fuel cells, *J. Electrochem. Soc.* 163 (2016) A5134–A5143. <https://doi.org/10.1149/2.0181601jes>.
- [123] G. Lin, P.Y. Chong, V. Yarlagadda, T.V. Nguyen, R.J. Wycisk, P.N. Pintauro, M. Bates, S. Mukerjee, M.C. Tucker, A.Z. Weber, Advanced hydrogen-bromine flow batteries with improved efficiency, durability and cost, *J. Electrochem. Soc.* 163 (2016) A5049–A5056. <https://doi.org/10.1149/2.0071601jes>.
- [124] L. Zhang, X. Wang, S. Wu, Z.G. Shao, S. Liu, H. Wang, A. Chen, Characterization and optimization of graphite felt/BP2000 composite electrode for the H<sub>2</sub>/Br<sub>2</sub> fuel cell, *RSC Adv.* 6 (2016) 12669–12675. <https://doi.org/10.1039/c5ra28015j>.
- [125] B. Duman, B. Fıçıcılar, Acid modified graphite felt cathode electrode for low temperature H<sub>2</sub>/Br<sub>2</sub> redox flow battery, *Res. Eng. Struct. Mater.* 6 (2020) 375–384. <https://doi.org/http://dx.doi.org/10.17515/resm2019.170en1217>.
- [126] R.S. Yeo, D.T. Chin, A hydrogen- bromine cell for energy storage applications, *J. Electrochem. Soc.* 127 (1980) 549–555. <https://doi.org/10.1149/1.2129710>.
- [127] G.G. Barna, S.N. Frank, T.H. Teherani, L.D. Weedon, Lifetime studies in H<sub>2</sub>/Br<sub>2</sub> fuel cells, *J. Electrochem. Soc.* 131 (1984) 1973–1980. <https://doi.org/10.1149/1.2116003>.
- [128] V. Livshits, A. Ulus, E. Peled, High-power H<sub>2</sub>/Br<sub>2</sub> fuel cell, *Electrochem. Commun.* 8 (2006) 1358–1362. <https://doi.org/10.1016/j.elecom.2006.06.021>.
- [129] H. Kreutzer, V. Yarlagadda, T. Van Nguyen, Performance evaluation of a regenerative hydrogen-bromine fuel cell, *J. Electrochem. Soc.* 159 (2012) F331–F337. <https://doi.org/10.1149/2.086207jes>.
- [130] K.T. Cho, P. Albertus, V. Battaglia, A. Kojic, V. Srinivasan, A.Z. Weber, Optimization and analysis of high-power hydrogen/bromine flow batteries for grid-scale energy storage, *Energy Technol.* 1 (2013) 596–608. <https://doi.org/10.1002/ente.201300108>.
- [131] M.C. Tucker, K.T. Cho, F.B. Spingler, A.Z. Weber, G. Lin, Impact of membrane characteristics on the performance and cycling of the Br<sub>2</sub>-H<sub>2</sub> redox flow cell, *J. Power Sources.* 284 (2015) 212–221. <https://doi.org/10.1016/j.jpowsour.2015.03.010>.
- [132] H. Prifti, A. Parasuraman, S. Winardi, T.M. Lim, M. Skyllas-Kazacos, Membranes for redox flow battery applications, *Membranes.* 2 (2012) 275–306. <https://doi.org/10.3390/membranes2020275>.
- [133] J.W. Park, R. Wycisk, P.N. Pintauro, Nafion/PVDF nanofiber composite membranes for regenerative hydrogen/bromine fuel cells, *J. Memb. Sci.* 490 (2015) 103–112. <https://doi.org/10.1016/j.memsci.2015.04.044>.
- [134] J. Woo Park, R. Wycisk, G. Lin, P. Ying Chong, D. Powers, T. Van Nguyen,

- R.P. Dowd, P.N. Pintauro, Electrospun Nafion/PVDF single-fiber blended membranes for regenerative H<sub>2</sub>/Br<sub>2</sub> fuel cells, *J. Memb. Sci.* 541 (2017) 85–92. <https://doi.org/10.1016/j.memsci.2017.06.086>.
- [135] V. Yarlagadda, R.P. Dowd, J.W. Park, P.N. Pintauro, T. Van Nguyen, A comprehensive study of an acid-based reversible H<sub>2</sub>-Br<sub>2</sub> fuel cell system, *J. Electrochem. Soc.* 162 (2015) F919–F926. <https://doi.org/10.1149/2.1041508jes>.
- [136] J.W. Park, R. Wycisk, P.N. Pintauro, V. Yarlagadda, T. Van Nguyen, Electrospun Nafion<sup>®</sup>/polyphenylsulfone composite membranes for regenerative hydrogen bromine fuel cells, *Materials*. 9 (2016). <https://doi.org/10.3390/ma9030143>.
- [137] W.A. Braff, M.Z. Bazant, C.R. Buie, Membrane-less hydrogen bromine flow battery, *Nat. Commun.* 4 (2013) 2346. <https://doi.org/10.1038/ncomms3346>.
- [138] D. Alfisi, A.N. Shocron, R. Gloukhovski, D.A. Vermaas, M.E. Suss, Resistance breakdown of a membraneless hydrogen-bromine redox flow battery, *ACS Sustain. Chem. Eng.* 10 (2022) 12985–12992. <https://doi.org/10.1021/acssuschemeng.2c02169>.
- [139] R.J. Remick, P.G.P. Ang, Electrically rechargeable anionically active reduction-oxidation electrical storage-supply system, US Patent 4485154 (1984).
- [140] F. Pan, Q. Wang, Redox species of redox flow batteries: A review, *Molecules*. 20 (2015) 20499–20517. <https://doi.org/10.3390/molecules201119711>.
- [141] P. Morrissey, Regenesys: A new energy storage technology, *Int. J. Ambient Energy*. 21 (2000) 213–220. <https://doi.org/10.1080/01430750.2000.9675376>.
- [142] S.H. Ge, B.L. Yi, H.M. Zhang, Study of a high power density sodium polysulfide/bromine energy storage cell, *J. Appl. Electrochem.* 34 (2004) 181–185. <https://doi.org/10.1023/B:JACH.0000009936.82613.ad>.
- [143] P. Zhao, H. Zhang, H. Zhou, B. Yi, Nickel foam and carbon felt applications for sodium polysulfide/bromine redox flow battery electrodes, *Electrochim. Acta*. 51 (2005) 1091–1098. <https://doi.org/10.1016/j.electacta.2005.06.008>.
- [144] H. Zhou, H. Zhang, P. Zhao, Novel cobalt coated carbon felt as high performance negative electrode in sodium polysulfide/bromine redox flow battery, *Electrochemistry*. 74 (2006) 296–298. <https://doi.org/10.5796/electrochemistry.74.296>.
- [145] H. Zhou, H. Zhang, P. Zhao, B. Yi, A comparative study of carbon felt and activated carbon based electrodes for sodium polysulfide/bromine redox flow battery, *Electrochim. Acta*. 51 (2006) 6304–6312. <https://doi.org/10.1016/j.electacta.2006.03.106>.
- [146] D.P. Scamman, G.W. Reade, E.P.L. Roberts, Numerical modelling of a bromide-polysulphide redox flow battery. Part 2: Evaluation of a utility-scale system, *J. Power Sources*. 189 (2009) 1231–1239. <https://doi.org/10.1016/j.jpowsour.2009.01.076>.
- [147] D.P. Scamman, G.W. Reade, E.P.L. Roberts, Numerical modelling of a bromide-polysulphide redox flow battery. Part 1: Modelling approach and

- validation for a pilot-scale system, *J. Power Sources*. 189 (2009) 1220–1230. <https://doi.org/10.1016/j.jpowsour.2009.01.071>.
- [148] M. Skyllas-Kazacos, Novel vanadium chloride/polyhalide redox flow battery, *J. Power Sources*. 124 (2003) 299–302. [https://doi.org/10.1016/S0378-7753\(03\)00621-9](https://doi.org/10.1016/S0378-7753(03)00621-9).
- [149] X. Rui, M.O. Oo, D.H. Sim, S.C. Raghu, Q. Yan, T.M. Lim, M. Skyllas-Kazacos, Graphene oxide nanosheets/polymer binders as superior electrocatalytic materials for vanadium bromide redox flow batteries, *Electrochim. Acta*. 85 (2012) 175–181. <https://doi.org/10.1016/j.electacta.2012.08.119>.
- [150] X. Rui, A. Parasuraman, W. Liu, D.H. Sim, H.H. Hng, Q. Yan, T.M. Lim, M. Skyllas-Kazacos, Functionalized single-walled carbon nanotubes with enhanced electrocatalytic activity for  $\text{Br}^-/\text{Br}_3^-$  redox reactions in vanadium bromide redox flow batteries, *Carbon*. 64 (2013) 464–471. <https://doi.org/10.1016/j.carbon.2013.07.099>.
- [151] G. Poon, A. Parasuraman, T.M. Lim, M. Skyllas-Kazacos, Evaluation of N-ethyl-N-methyl-morpholinium bromide and N-ethyl-N-methyl-pyrrolidinium bromide as bromine complexing agents in vanadium bromide redox flow batteries, *Electrochim. Acta*. 107 (2013) 388–396. <https://doi.org/10.1016/j.electacta.2013.06.084>.
- [152] D. Kim, Y. Kim, Y. Lee, J. Jeon, 1,2-Dimethylimidazole based bromine complexing agents for vanadium bromine redox flow batteries, *Int. J. Hydrogen Energy*. 44 (2019) 12024–12032. <https://doi.org/10.1016/j.ijhydene.2019.03.050>.
- [153] H. Vafiadis, M. Skyllas-Kazacos, Evaluation of membranes for the novel vanadium bromine redox flow cell, *J. Memb. Sci.* 279 (2006) 394–402. <https://doi.org/10.1016/j.memsci.2005.12.028>.
- [154] M. Skyllas-Kazacos, N. Milne, G.C. Kazacos, Membrane properties and behaviour in the generation 2 vanadium bromide redox flow batteries, *Mater. Forum*. 32 (2007) 72–77.
- [155] S. Winardi, S.C. Raghu, M.O. Oo, Q. Yan, N. Wai, T.M. Lim, M. Skyllas-Kazacos, Sulfonated poly (ether ether ketone)-based proton exchange membranes for vanadium redox battery applications, *J. Memb. Sci.* 450 (2014) 313–322. <https://doi.org/10.1016/j.memsci.2013.09.024>.
- [156] M. Park, J. Ryu, W. Wang, J. Cho, Material design and engineering of next-generation flow-battery technologies, *Nat. Rev. Mater.* 2 (2016) 1–18. <https://doi.org/10.1038/natrevmats.2016.80>.
- [157] M. Quan, D. Sanchez, M.F. Wasylkiw, D.K. Smith, Voltammetry of quinones in unbuffered aqueous solution: Reassessing the roles of proton transfer and hydrogen bonding in the aqueous electrochemistry of quinones, *J. Am. Chem. Soc.* 129 (2007) 12847–12856. <https://doi.org/10.1021/ja0743083>.
- [158] Z. Yang, L. Tong, D.P. Tabor, E.S. Beh, M-A Goulet, D. De Porcellinis, A. Aspuru-guzik, R.G. Gordon, M.J. Aziz, Alkaline benzoquinone aqueous flow battery for large- scale storage of electrical energy, *Adv. Energy Mater.* 8

- (2018) 1702056. <https://doi.org/10.1002/aenm.201702056>.
- [159] B. Huskinson, M.P. Marshak, C. Suh, S. Er, M.R. Gerhardt, C.J. Galvin, X. Chen, A. Aspuru-Guzik, R.G. Gordon, M.J. Aziz, A metal-free organic-inorganic aqueous flow battery, *Nature*. 505 (2014) 195–198. <https://doi.org/10.1038/nature12909>.
- [160] B. Huskinson, M.P. Marshak, M.R. Gerhardt, M.J. Aziz, Cycling of a quinone-bromide flow battery for large-scale electrochemical energy storage, *ECS Trans.* 61 (2014) 27–30. <https://doi.org/10.1149/06137.0027ecst>.
- [161] Q. Chen, M.R. Gerhardt, L. Hartle, M.J. Aziz, A quinone-bromide flow battery with 1 W/cm<sup>2</sup> power density, *J. Electrochem. Soc.* 163 (2016) A5010–A5013. <https://doi.org/10.1149/2.0021601jes>.
- [162] M.R. Gerhardt, L. Tong, R. Gómez-Bombarelli, Q. Chen, M.P. Marshak, C.J. Galvin, A. Aspuru-Guzik, R.G. Gordon, M.J. Aziz, Anthraquinone derivatives in aqueous flow batteries, *Adv. Energy Mater.* 7 (2017) 1601488. <https://doi.org/10.1002/aenm.201601488>.
- [163] A. Khataee, K. Wedege, E. Dražević, A. Bentien, Differential pH as a method for increasing cell potential in organic aqueous flow batteries, *J. Mater. Chem. A*. 5 (2017) 21875–21882. <https://doi.org/10.1039/c7ta04975g>.
- [164] A. Khataee, E. Dražević, J. Catalano, A. Bentien, Performance optimization of differential pH quinone-bromide redox flow battery, *J. Electrochem. Soc.* 165 (2018) A3918–A3924. <https://doi.org/10.1149/2.0681816jes>.
- [165] J. Luo, W. Wu, C. Debruler, B. Hu, M. Hu, T.L. Liu, A 1.51 V pH neutral redox flow battery towards scalable energy storage, *J. Mater. Chem. A*. 7 (2019) 9130–9136. <https://doi.org/10.1039/c9ta01469a>.
- [166] W. Liu, Y. Liu, H. Zhang, C. Xie, L. Shi, Y.G. Zhou, X. Li, A highly stable neutral viologen/bromine aqueous flow battery with high energy and power density, *Chem. Commun.* 55 (2019) 4801–4804. <https://doi.org/10.1039/c9cc00840c>.
- [167] B. Ambrose, R. Naresh, M. Kathiresan, M. Ulaganathan, P. Ragupathy, Highly stable asymmetric viologen as an anolyte for aqueous organic and halide based redox flow batteries, *Energy Technol.* 2201046 (2022) 1–8. <https://doi.org/10.1002/ente.202201046>.
- [168] Y. Zhao, Y. Ding, J. Song, L. Peng, J.B. Goodenough, G. Yu, A reversible Br<sub>2</sub>/Br<sup>−</sup> redox couple in the aqueous phase as a high-performance catholyte for alkali-ion batteries, *Energy Environ. Sci.* 7 (2014) 1990–1995. <https://doi.org/10.1039/C4EE00407H>.
- [169] S. Das, S. Voskian, K.P. Rajczykowski, T.A. Hatton, M.Z. Bazant, Enabling a stable high-power lithium-bromine flow battery using task-specific ionic liquids, *J. Electrochem. Soc.* 168 (2021) 070542. <https://doi.org/10.1149/1945-7111/ac1396>.
- [170] P. Bai, V. Viswanathan, M.Z. Bazant, A dual-mode rechargeable lithium-bromine/oxygen fuel cell, *J. Mater. Chem. A*. 3 (2015) 14165–14172. <https://doi.org/10.1039/c5ta03335g>.
- [171] P. Bai, M.Z. Bazant, Performance and degradation of a lithium-bromine



- rechargeable fuel cell using highly concentrated catholytes, *Electrochim. Acta*. 202 (2016) 216–223. <https://doi.org/10.1016/j.electacta.2016.04.010>.
- [172] Y. Zeng, Z. Yang, F. Lu, Y. Xie, A novel tin-bromine redox flow battery for large-scale energy storage, *Appl. Energy*. 255 (2019) 113756. <https://doi.org/10.1016/j.apenergy.2019.113756>.
- [173] X. Li, C. Xie, T. Li, Y. Zhang, X. Li, Low-cost titanium-bromine flow battery with ultrahigh cycle stability for grid-scale energy storage, *Adv. Mater.* 32 (2020) 1–8. <https://doi.org/10.1002/adma.202005036>.
- [174] Y. Xu, C. Xie, X. Li, Bromine-graphite intercalation enabled two-electron transfer for a bromine-based flow battery, *Trans. Tianjin Univ.* 28 (2022) 186–192. <https://doi.org/10.1007/s12209-022-00327-w>.
- [175] D. Lin, Y. Li, Recent advances of aqueous rechargeable zinc-iodine batteries: challenges, solutions, and prospects, *Adv. Mater.* 34 (2022) 1–28. <https://doi.org/10.1002/adma.202108856>.
- [176] Z. Li, G. Weng, Q. Zou, G. Cong, Y.C. Lu, A high-energy and low-cost polysulfide/iodide redox flow battery, *Nano Energy*. 30 (2016) 283–292. <https://doi.org/10.1016/j.nanoen.2016.09.043>.
- [177] W. Liu, W. Lu, H. Zhang, X. Li, Aqueous flow batteries: research and development, *Chem. Eur. J.* 25 (2019) 1649–1664. <https://doi.org/10.1002/chem.201802798>.
- [178] L. Su, A.F. Badel, C. Cao, J.J. Hinricher, F.R. Brushett, Toward an inexpensive aqueous polysulfide-polyiodide redox flow battery, *Ind. Eng. Chem. Res.* 56 (2017) 9783–9792. <https://doi.org/10.1021/acs.iecr.7b01476>.
- [179] D. Ma, B. Hu, W. Wu, X. Liu, J. Zai, C. Shu, T. Tadesse Tsega, L. Chen, X. Qian, T.L. Liu, Highly active nanostructured CoS<sub>2</sub>/CoS heterojunction electrocatalysts for aqueous polysulfide/iodide redox flow batteries, *Nat. Commun.* 10 (2019) 3367. <https://doi.org/10.1038/s41467-019-11176-y>.
- [180] Y. Qin, X. Li, W. Liu, X. Lei, High-performance aqueous polysulfide-iodide flow battery realized by an efficient bifunctional catalyst based on copper sulfide, *Mater. Today Energy*. 21 (2021). <https://doi.org/10.1016/j.mtener.2021.100746>.
- [181] J. Liu, L. Ren, Y. Wang, X. Lu, M. Zhou, W. Liu, A highly-stable bifunctional NiCo<sub>2</sub>S<sub>4</sub> nanoarray@carbon paper electrode for aqueous polysulfide/iodide redox flow battery, *J. Power Sources*. 561 (2023) 232607. <https://doi.org/10.1016/j.jpowsour.2022.232607>.
- [182] M. Rahimi, A. Molaei Dehkordi, H. Gharibi, E.P.L. Roberts, Novel magnetic flowable electrode for redox flow batteries: a polysulfide/iodide case study, *Ind. Eng. Chem. Res.* 60 (2021) 824–841. <https://doi.org/10.1021/acs.iecr.0c05768>.
- [183] M. Rahimi, A. Molaei Dehkordi, E.P.L. Roberts, Magnetic nanofluidic electrolyte for enhancing the performance of polysulfide/iodide redox flow batteries, *Electrochim. Acta*. 369 (2021) 137687. <https://doi.org/10.1016/j.electacta.2020.137687>.
- [184] Z. Li, Y.C. Lu, Polysulfide-based redox flow batteries with long life and low leveled cost enabled by charge-reinforced ion-selective membranes, *Nat.*

- Energy. 6 (2021) 517–528. <https://doi.org/10.1038/s41560-021-00804-x>.
- [185] B. Li, Z. Nie, M. Vijayakumar, G. Li, J. Liu, V. Sprenkle, W. Wang, Ambipolar zinc-polyiodide electrolyte for a high-energy density aqueous redox flow battery, *Nat. Commun.* 6 (2015). <https://doi.org/10.1038/ncomms7303>.
- [186] B. Li, J. Liu, Z. Nie, W. Wang, D. Reed, J. Liu, P. McGrail, V. Sprenkle, Metal-organic frameworks as highly active electrocatalysts for high-energy density, aqueous zinc-polyiodide redox flow batteries, *Nano Lett.* 16 (2016) 4335–4340. <https://doi.org/10.1021/acs.nanolett.6b01426>.
- [187] W.J. Jang, J.S. Cha, H. Kim, J.H. Yang, Effect of an iodine film on charge-transfer resistance during the electro-oxidation of iodide in redox flow batteries, *ACS Appl. Mater. Interfaces.* 13 (2021) 6385–6393. <https://doi.org/10.1021/acsami.0c22895>.
- [188] Y. Zhao, Y. Li, J. Mao, Z. Yi, N. Mubarak, Y. Zheng, J-K. Kim, Q. Chen, Accelerating the dissolution kinetics of iodine with a cosolvent for a high-current zinc-iodine flow battery, *J. Mater. Chem. A.* (2022) 14090–14097. <https://doi.org/10.1039/d2ta03195g>.
- [189] J. Yang, Y. Song, Q. Liu, A. Tang, High-capacity zinc-iodine flow batteries enabled by a polymer-polyiodide complex cathode, *J. Mater. Chem. A.* 9 (2021) 16093–16098. <https://doi.org/10.1039/d1ta03905a>.
- [190] J. Wu, Q. Dai, H. Zhang, X. Li, A defect-free MOF composite membrane prepared via in-situ binder-controlled restrained second-growth method for energy storage device, *Energy Storage Mater.* 35 (2021) 687–694. <https://doi.org/10.1016/j.ensm.2020.11.040>.
- [191] L. Gao, Y. Ding, G. He, G. Yu, Bio-derived and cost-effective membranes with high selectivity for redox flow batteries based on host-guest chemistry, *Small.* 18 (2022) 1–7. <https://doi.org/10.1002/sml.202107055>.
- [192] C. Xie, H. Zhang, W. Xu, W. Wang, X. Li, A long cycle life, self-healing zinc-iodine flow battery with high power density, *Angew. Chem.* 57 (2018) 11171–11176. <https://doi.org/10.1002/anie.201803122>.
- [193] G.M. Weng, Z. Li, G. Cong, Y. Zhou, Y.C. Lu, Unlocking the capacity of iodide for high-energy-density zinc/polyiodide and lithium/polyiodide redox flow batteries, *Energy Environ. Sci.* 10 (2017) 735–741. <https://doi.org/10.1039/c6ee03554j>.
- [194] Q.P. Jian, M.C. Wu, H.R. Jiang, Y.K. Lin, T.S. Zhao, A trifunctional electrolyte for high-performance zinc-iodine flow batteries, *J. Power Sources.* 484 (2021) 229238. <https://doi.org/10.1016/j.jpowsour.2020.229238>.
- [195] M. Mousavi, G. Jiang, J. Zhang, A.G. Kashkooli, H. Dou, C.J. Silva, Z.P. Cano, Y. Niu, A. Yu, Z. Chen, Decoupled low-cost ammonium-based electrolyte design for highly stable zinc-iodine redox flow batteries, *Energy Storage Mater.* 32 (2020) 465–476. <https://doi.org/10.1016/j.ensm.2020.06.031>.
- [196] J. Zhang, G. Jiang, P. Xu, A.G. Kashkooli, M. Mousavi, A. Yu, Z. Chen, An all-aqueous redox flow battery with unprecedented energy density, *Energy Environ. Sci.* 11 (2018) 2010–2015. <https://doi.org/10.1039/c8ee00686e>.
- [197] C. Xie, Y. Liu, W. Lu, H. Zhang, X. Li, Highly stable zinc-iodine single flow

- batteries with super high energy density for stationary energy storage, *Energy Environ. Sci.* 12 (2019) 1834–1839. <https://doi.org/10.1039/c8ee02825g>.
- [198] S. Ito, M. Sugimasa, Y. Toshimitsu, A. Orita, M. Kitagawa, M. Sakai, Formation of a hydrophobic polyiodide complex during cathodic oxidation of iodide in the presence of propylene carbonate in aqueous solutions, and its application to a zinc/iodine redox flow battery, *Electrochim. Acta.* 319 (2019) 164–174. <https://doi.org/10.1016/j.electacta.2019.06.150>.
- [199] Y. Yao, Z. Wang, Z. Li, Y.C. Lu, A dendrite-free tin anode for high-energy aqueous redox flow batteries, *Adv. Mater.* 33 (2021) 1–8. <https://doi.org/10.1002/adma.202008095>.
- [200] Y. Zhao, H.R. Byon, High-performance lithium-iodine flow battery, *Adv. Energy Mater.* 3 (2013) 1630–1635. <https://doi.org/10.1002/aenm.201300627>.
- [201] H. Chen, Y.C. Lu, A high-energy-density multiple redox semi-solid-liquid flow battery, *Adv. Energy Mater.* 6 (2016) 1–9. <https://doi.org/10.1002/aenm.201502183>.
- [202] Z. Wang, L.Y.S. Tam, Y.C. Lu, Flexible solid flow electrodes for high-energy scalable energy storage, *Joule.* 3 (2019) 1677–1688. <https://doi.org/10.1016/j.joule.2019.05.015>.
- [203] Z. Liang, Y.C. Lu, Critical role of redox mediator in suppressing charging instabilities of lithium-oxygen batteries, *J. Am. Chem. Soc.* 138 (2016) 7574–7583. <https://doi.org/10.1021/jacs.6b01821>.
- [204] T. Liu, M. Leskes, W. Yu, A.J. Moore, L. Zhou, P.M. Bayley, G. Kim, C.P. Grey, Cycling Li-O<sub>2</sub> batteries via LiOH formation and decomposition, *Science.* 350 (2015) 530–533. <https://doi.org/10.1126/science.aac7730>.
- [205] X. Zheng, Y. Wang, Y. Xu, T. Ahmad, Y. Yuan, J. Sun, R. Luo, M. Wang, M. Chuai, N. Chen, T. Jiang, S. Liu, W. Chen, Boosting electrolytic MnO<sub>2</sub>-Zn batteries by a bromine mediator, *Nano Lett.* 21 (2021) 8863–8871. <https://doi.org/10.1021/acs.nanolett.1c03319>.
- [206] Y. Liu, C. Xie, X. Li, Bromine assisted MnO<sub>2</sub> dissolution chemistry: Toward a hybrid flow battery with energy density of over 300 Wh L<sup>-1</sup>, *Angew. Chem.* 61 (2022). <https://doi.org/10.1002/anie.202213751>.
- [207] M. Liu, Y.X. Ren, H.R. Jiang, C. Luo, F.Y. Kang, T.S. Zhao, An efficient Li<sub>2</sub>S-based lithium-ion sulfur battery realized by a bifunctional electrolyte additive, *Nano Energy.* 40 (2017) 240–247. <https://doi.org/10.1016/j.nanoen.2017.08.017>.
- [208] T. Shiga, H. Kondo, Y. Kato, Y. Hase, Iodine mediator with anomalously high redox potential and its application to a catalytic cycle for lithium carbonate decomposition toward future lithium reproduction, *J. Phys. Chem. C.* 123 (2019) 3944–3950. <https://doi.org/10.1021/acs.jpcc.8b09967>.
- [209] L. Hu, T. Zhai, H. Li, Y. Wang, Redox-mediator-enhanced electrochemical capacitors: Recent advances and future perspectives, *ChemSusChem.* 12 (2019) 1118–1132. <https://doi.org/10.1002/cssc.201802450>.
- [210] B. V. Bergeron, A. Marton, G. Oskam, G.J. Meyer, Dye-sensitized SnO<sub>2</sub> electrodes with iodide and pseudohalide redox mediators, *J. Phys. Chem. B.*

- 109 (2005) 937–943. <https://doi.org/10.1021/jp0461347>.
- [211] F. Zhang, M. Gao, S. Huang, H. Zhang, X. Wang, L. Liu, M. Han, Q. Wang, Redox targeting of energy materials for energy storage and conversion, *Adv. Mater.* 34 (2022) 1–19. <https://doi.org/10.1002/adma.202104562>.
- [212] Q. Huang, J. Yang, C.B. Ng, C. Jia, Q. Wang, A redox flow lithium battery based on the redox targeting reactions between  $\text{LiFePO}_4$  and iodide, *Energy Environ. Sci.* 9 (2016) 917–921. <https://doi.org/10.1039/c5ee03764f>.
- [213] J. Lei, Y. Yao, Z. Wang, Y.C. Lu, Towards high-areal-capacity aqueous zinc-manganese batteries: Promoting  $\text{MnO}_2$  dissolution by redox mediators, *Energy Environ. Sci.* 14 (2021) 4418–4426. <https://doi.org/10.1039/d1ee01120k>.
- [214] Z. Yu, N. Vlachopoulos, M. Gorlova, L. Kloo, Liquid electrolytes for dye-sensitized solar cells, *Dalt. Trans.* 40 (2011) 10311–10315. <https://doi.org/10.1039/c1dt11184a>.
- [215] M. Yu, W.D. McCulloch, D.R. Beauchamp, Z. Huang, X. Ren, Y. Wu, Aqueous lithium-iodine solar flow battery for the simultaneous conversion and storage of solar energy, *J. Am. Chem. Soc.* 137 (2015) 8332–8335. <https://doi.org/10.1021/jacs.5b03626>.
- [216] J. Ma, M. Liu, Y. He, J. Zhang, Iodine redox chemistry in rechargeable batteries, *Angew. Chem.* 133 (2021) 12744–12755. <https://doi.org/10.1002/ange.202009871>.
- [217] L. Fan, C. Jia, Y.G. Zhu, Q. Wang, Redox targeting of prussian blue: Toward low-cost and high energy density redox flow battery and solar rechargeable battery, *ACS Energy Lett.* 2 (2017) 615–621. <https://doi.org/10.1021/acsenenergylett.6b00667>.
- [218] Q. Huang, Q. Wang, Next-generation, high-energy-density redox flow batteries, *Chempluschem.* 80 (2015) 312–322. <https://doi.org/10.1002/cplu.201402099>.
- [219] G.C. Hayward, P.J. Hendra, The far infra-red and Raman spectra of the trihalide ions  $\text{IBr}_2^-$  and  $\text{I}_3^-$ , *Spectrochim. Acta Part A Mol. Spectrosc.* 23 (1967) 2309–2314. [https://doi.org/10.1016/0584-8539\(67\)80124-7](https://doi.org/10.1016/0584-8539(67)80124-7).
- [220] C. Park, J. Chang, Understanding the role of  $\text{Br}^-$  during the electrooxidation of  $\text{I}^-$  in aqueous media:  $\text{I}_2\text{Br}(\text{aq})$ -formation without the precipitation of an iodine film, *Bull. Korean Chem. Soc.* 42 (2021) 1678. <https://doi.org/10.1002/bkcs.12406>.
- [221] M. Skyllas-Kazacos, N. Milne, Evaluation of iodide and titanium halide redox couple combinations for common electrolyte redox flow cell systems, *J. Appl. Electrochem.* 41 (2011) 1233–1243. <https://doi.org/10.1007/s10800-011-0287-y>.
- [222] L. Li, S. Kim, W. Wang, M. Vijayakumar, Z. Nie, B. Chen, J. Zhang, G. Xia, J. Hu, G. Graff, J. Liu, Z. Yang, A stable vanadium redox-flow battery with high energy density for large-scale energy storage, *Adv. Energy Mater.* 1 (2011) 394–400. <https://doi.org/10.1002/aenm.201100008>.
- [223] M. Vijayakumar, W. Wang, Z. Nie, V. Sprenkle, J. Hu, Elucidating the higher stability of vanadium(V) cations in mixed acid based redox flow battery

- electrolytes, *J. Power Sources*. 241 (2013) 173–177. <https://doi.org/10.1016/j.jpowsour.2013.04.072>.
- [224] S. Kim, M. Vijayakumar, W. Wang, J. Zhang, B. Chen, Z. Nie, F. Chen, J. Hu, L. Li, Z. Yang, Chloride supporting electrolytes for all-vanadium redox flow batteries, *Phys. Chem. Chem. Phys.* 13 (2011) 18186–18193. <https://doi.org/10.1039/c1cp22638j>.
- [225] Y. Yang, Y. Zhang, T. Liu, J. Huang, Improved broad temperature adaptability and energy density of vanadium redox flow battery based on sulfate-chloride mixed acid by optimizing the concentration of electrolyte, *J. Power Sources*. 415 (2019) 62–68. <https://doi.org/10.1016/j.jpowsour.2019.01.049>.
- [226] Z.H. Zhang, L. Wei, M.C. Wu, B.F. Bai, T.S. Zhao, Chloride ions as an electrolyte additive for high performance vanadium redox flow batteries, *Appl. Energy*. 289 (2021). <https://doi.org/10.1016/j.apenergy.2021.116690>.
- [227] G. Lacarbonara, L. Faggiano, S. Porcu, P.C. Ricci, S. Rapino, D.P. Casey, J.F. Rohan, C. Arbizzani, Copper chloro-complexes concentrated solutions: An electrochemical study, *Batteries*. 7 (2021) 1–16. <https://doi.org/10.3390/batteries7040083>.
- [228] L. Sanz, J. Palma, E. García-Quismondo, M. Anderson, The effect of chloride ion complexation on reversibility and redox potential of the Cu(II)/Cu(I) couple for use in redox flow batteries, *J. Power Sources*. 224 (2013) 278–284. <https://doi.org/10.1016/j.jpowsour.2012.10.005>.
- [229] G. Lacarbonara, N. Albanelli, D. Fazzi, C. Arbizzani, A spectroelectrochemical study of copper chloro-complexes for high performance all-copper redox flow batteries, *Electrochim. Acta*. 458 (2023) 1–9. <https://doi.org/10.1016/j.electacta.2023.142514>.
- [230] J. Wu, J. Yang, Z.Y. Leong, F. Zhang, H. Deng, G.F. Ouyang, J. Yu, A method to inhibit disproportionation of  $Mn^{3+}$  for low-cost Mn-Fe all-flow battery, *ACS Appl. Energy Mater.* 5 (2022) 14646–14651. <https://doi.org/10.1021/acsaem.2c03075>.
- [231] M. Yang, Z. Xu, W. Xiang, H. Xu, M. Ding, L. Li, A. Tang, R. Gao, G. Zhou, C. Jia, High performance and long cycle life neutral zinc-iron flow batteries enabled by zinc-bromide complexation, *Energy Storage Mater.* 44 (2022) 433–440. <https://doi.org/10.1016/j.ensm.2021.10.043>.